ADVANCES IN FOOD AND NUTRITION RESEARCH, VOL. 39

THE RHEOLOGY OF SEMILIQUID FOODS

GUSTAVO V. BARBOSA-CÁNOVAS

Biological Systems Engineering
Washington State University
Pullman, Washington 99164-6120

JOZEF L. KOKINI

Center for Advanced Foods
The State University of New Jersey
New Brunswick, New Jersey 08903

LI MA

Biological Systems Engineering
Washington State University
Pullman, Washington 99164-6120

ALBERT IBARZ

Food Technology
University of Lleida
25006 Lleida, Spain

I. INTRODUCTION

Food rheology is the study of the manner in which food materials respond to an applied stress or strain. The science of rheology has many applications in the fields of food acceptability, food processing, and food handling. Determination of rheological properties of foodstuffs provides an instrumental quality control of raw material prior to processing, of intermediate products during manufacturing, and of finished goods after production. Determination of rheological properties of foodstuffs is also useful in elucidation of structure and composition of food and analysis of structural changes during processing (Escher, 1983).

The rheological properties of foodstuffs are important in food process engineering since they are the essential parameters in plant design (pumping requirements, pipe and valve dimensions, and mixing operations, etc.) and in the calculation of basic heat, mass, and momentum transfer (Szczesniak, 1977).

Instrumental quality control before, during, and after manufacture is one area to which food rheology makes important contributions. For example, the measurement of apparent viscosity and yield stress of ketchup helps to predict how well tomato ketchup drains from a bottle. A number of tests have been developed using either basic rheological instruments (rotational viscometer, capillary viscometers, etc.) or instruments simulating the situation in which the rheological properties are of importance (Bostwick

Consistometer) (Gould, 1983; Harper, 1960; Rao *et al.,* 1981; Rao and Cooley, 1983; Rani and Bains, 1987).

Rheological quality control measurements are also used to follow changes in foods during processing and storage. For instance, in manufacturing an apple nectar beverage by enzymatic breakdown of apple pulp, Struebi *et al.* (1978) measured flow curves after various lengths of treatment. An optimum suspension stability and consumer-determined quality of the final beverage can be achieved by monitoring viscosity in the pulp liquefying process. The chemical analysis of changes in pectic substances and other cell wall material of the apple tissue was much more difficult and did not yield a conclusive picture as to how far these substances had to be enzymatically altered for optimum quality.

In sensory evaluation consumers estimate fruit firmness on the basis of the deformation resulting from physical pressure applied by the hand and fingers. The toughness or tenderness of meat is subjectively evaluated in terms of the effort required for the teeth to penetrate and masticate the flesh tissues. Therefore, determination of rheological properties of foodstuffs is important in evaluation of consumer-determined quality by correlating rheological measurements with sensory tests.

Foods, however, are complex materials structurally and rheologically. In many instances they consist of mixtures of solid as well as fluid structural components, e.g., solid cellwall material, water and colloidal liquids, and intercellular gases. Many foodstuffs are neither homogeneous nor isotropic and have properties which vary from one point to another within their mass. All these complicating factors make the study of food rheology more difficult than the study of rheology in other fields such as polymer rheology. Nevertheless, investigators report that many foods do behave in a predictable manner and that concepts from elasticity, viscosity, and viscoelasticity theories can be used to interpret their response to applied deformation or applied force. In this review, the basic food rheology concepts such as shear rate, shear stress, viscosity, elasticity, and viscoelasticity are introduced; the experimental methods for steady shear; extensional flow, and dynamic measurements are described; the principles of instrumentation are discussed; constitutive models based on steady shear flow, diluted solution molecular theories, and concentrate solutions are presented; and applications of rheology in characterizing engineering properties of foods are reviewed.

II. BASIC RHEOLOGY CONCEPTS

Food rheology is concerned with the description of the mechanical properties of food materials under various deformation conditions. To under-

stand and use rheological information it is essential to have a mechanistic basis for the interpretation and correlation of the experimental data. Such interpretation of behavior in terms of theoretical mechanisms provides the guidelines needed to make sense of observations, to relate behavior to composition and structure, to predict and to modify properties, and to compare one experimental method with another. Under external force, the food materials exhibit the ability to flow, or accumulate recoverable deformations, or both. According to the extent of recoverable deformation, the basic rheology concepts can be classified into viscous flow, elastic deformation, and viscoelasticity.

A. VISCOUS FLOW

Viscosity is a measure of a fluid's ability to resist motion when a shearing stress is applied. Considering a simple geometry (Fig. 1), the upper plate is caused to move with a velocity (v) relative to the lower plate. This velocity is due to the application of a shearing force (F) per unit area. The layers of fluid contacting the plates are considered to move at the same velocities as the surface they contact; i.e., the assumption is made that no slipping occurs at the walls. The fluid then behaves as a series of parallel layers, or lamina, whose velocities are proportional to their distance from the lower plate. The differentiation of velocity with respect to the distance (dv/dy) is defined as shear rate

$$\dot{\gamma} \equiv -\frac{dv}{dy}. \tag{1}$$

For a class of fluid known as Newtonian fluid, there is a linear relationship between shear stress and shear rate. The dynamic viscosity (or coefficient of viscosity) is defined as the ratio of the shear stress to the shear rate

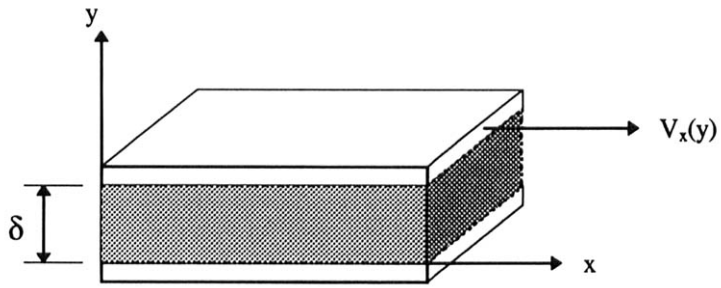

FIG. 1. Schematic diagram of flow induced by displacement of one of a pair of parallel planes.

$$\eta = \frac{\tau}{\dot{\gamma}} \tag{2a}$$

or

$$\tau = \eta\dot{\gamma}, \tag{2b}$$

where η is called Newtonian viscosity, $\dot{\gamma}$ is the shear strain rate or shear rate, and τ is the shear stress.

Curve a in Fig. 2 illustrates the relationship between the shear stress and shear rate of a Newtonian fluid. The plot is a straight line passing through the origin. The slope of the line is, by definition, the viscosity. However, most food materials are very complex (i.e., emulsions, suspension of solids, biopolymers such as carbohydrates, proteins, food gums, etc.), and their rheological behaviors do not obey Eq. (2). Instead, food materials exhibit either pseudoplastic (shear thinning) or dilatant (shear thickening) behavior. In these situations the viscosity is no longer constant, but dependent on the shear rate. The shear rate-dependent viscosity is called apparent viscosity (η_a). Curves b and c in Fig. 2 show the relationships between shear stress and shear rate for the shear thickening and shear thinning fluid behaviors, respectively. Compared to Newtonian fluid behavior (curve a), they either exhibit an upward or downward curvature. The typical equation to characterize the shear thickening and shear thinning fluid is the power law

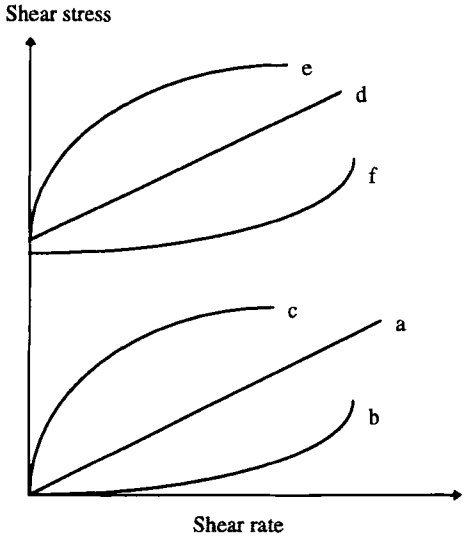

FIG. 2. Rheograms for time-independent fluids.

$$\tau = K\dot{\gamma}^n \tag{3a}$$

or

$$\eta_a = \frac{\tau}{\dot{\gamma}} = K\dot{\gamma}^{n-1}, \tag{3b}$$

where K is the consistence index (Pa · sec^n), n is flow index, and η_a is apparent viscosity (Pa · sec). When $n > 1$, the plot for shear stress–shear rate will be an upward curvature, which represents the shear thickening fluid; when $0 < n < 1$, the plot for the shear stress–shear rate will be a downward curvature, which represents the shear thinning fluid. When $n = 1$, Eq. (3) is reduced to Eq. (2) and represents the behavior of a Newtonian fluid.

Some other food materials exhibit a yield stress which may be defined as a minimum shear stress required to initiate flow. Although the existence of yield stress in fluids is still a controversial topic (Barnes and Walters, 1985; Cheng, 1986; Hartnett and Hu, 1989; Steffe, 1992a; Evans, 1992; Schurz, 1992), there is little doubt that yield stress is an engineering reality (Hartnett and Hu, 1989) which may strongly influence process calculations. Yield stress imparts stability to food emulsions in low-stress situations (e.g., during storage and transportation, where the stress involved is usually lower than the yield stress). The most common model for characterizing non-Newtonian fluids with yield stress is the Herschel–Bulkley equation

$$\tau = \tau_0 + K\dot{\gamma}^n \tag{4a}$$

or

$$\eta_a = \frac{\tau - \tau_0}{\dot{\gamma}} = K\dot{\gamma}^{n-1}, \tag{4b}$$

where τ is the shear stress, $\dot{\gamma}$ is the shear rate, n is the flow index, τ_0 is the yield stress, K is the consistency index, and η_a is apparent viscosity.

Based on the magnitude of n and τ_0, the non-Newtonian behavior can be classified as shear thinning, shear thickening, Bingham plastic, pseudoplastic with yield stress, or dilatant with yield stress (see Fig. 2 and Table I). The Herschel–Bulkley model is able to describe the general flow properties of fluid foods within a certain shear range. The discussion on this classification and examples of food materials has been reviewed by Sherman (1970), DeMan (1976), Barbosa-Cánovas and Peleg (1983), and Barbosa-Cánovas *et al.* (1993).

TABLE I

CLASSIFICATION OF NEWTONIAN AND NON-NEWTONIAN FLUIDS

	τ_0	n	K
Newtonian	0	1	$K = \eta$
Non-Newtonian			
Shear thinning (pseudoplastic)	0	$0 < n < 1$	>0
Shear thickening (dilatant)	0	$n > 1$	>0
Bingham	>0	1	>0
Pseudoplastic with yield stress	>0	$0 < n < 1$	>0
Dilatant with yield stress	>0	$n > 1$	>0

B. IDEAL ELASTIC BEHAVIOR (HOOKEAN BODY)

An ideal elastic body (also called Hooke's body) is defined as a material that deforms reversibly and for which the strain is proportional to the stress, with recovery to the original volume and shape occurring immediately upon release of the stress. In a Hooke body, stress is directly proportional to strain, as illustrated in Fig. 3. The relationship is known as Hooke's law, and the behavior is referred to as Hookean behavior.

Based on Hooke's law, the following relationships have been established for elastic, homogeneous, and isotropic materials under tensile or compressive stresses (see Fig. 4a)

$$E = \frac{\sigma}{\varepsilon}, \tag{5}$$

where E is the elastic modulus (or Young's modulus, Pa), σ is the tensile or compressive stress (Pa), and ε is the tensile or compressive strain [$\varepsilon = (L' - L)/L$, dimensionless].

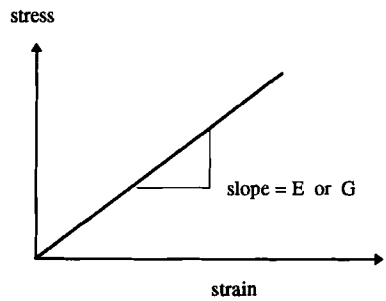

FIG. 3. Ideal elastic behavior.

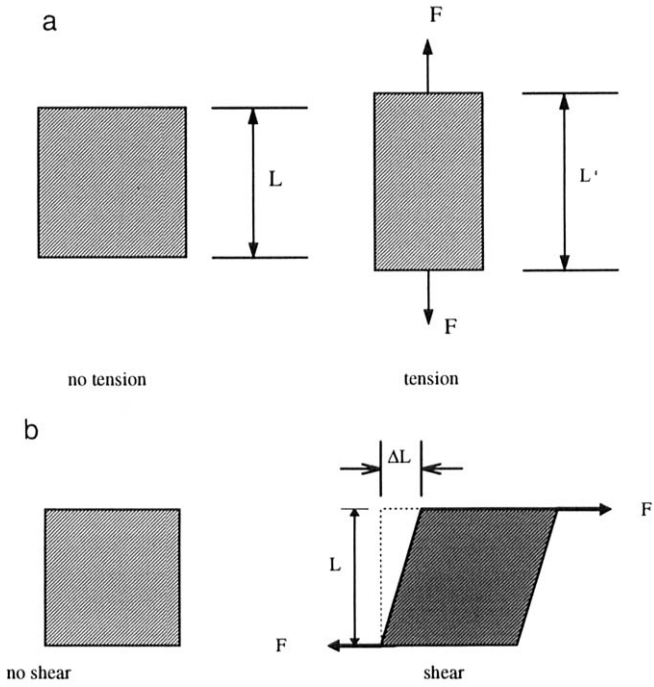

FIG. 4. Hooke's elasticity in (a) tension and (b) shear.

When the Hooke solid is subjected to distortion by shear stresses (Fig. 4b), the shear modulus or modulus of rigidity is given by

$$G = \frac{\tau}{\gamma}, \tag{6}$$

where G is shear modulus (Pa), τ is the shear stress (Pa), and γ is shear strain ($= \Delta L/L$, dimensionless).

C. TIME EFFECTS

Time-dependent rheological properties reflect the nature of a system's structure and can be due to viscoelasticity, structural changes, or both (Cheng and Evans, 1965; Harris, 1972). Structure breakdown can result in a decrease in the viscosity of a substance. It occurs in emulsions, suspensions, and sols. The characterization of the time-dependent flow properties of food systems is important for process design and control, for product devel-

opment, to establish relationships between structure and flow, and to correlate physical parameters with sensory evaluation.

Most foods exhibit time-dependent rheological properties (Rha, 1978; Shama and Sherman, 1966; Tiu and Boger, 1974; Mitchell, 1979; Bloksma, 1972; Peleg, 1977; Dickie and Kokini, 1982). The classical approach to characterize structural breakdown is the measurement of the hysteresis loop, first reported by Green and Weltmann (1943). A sample is sheared at a continuously increasing, then continuously decreasing shear rate, and a shear stress–shear rate flow curve is plotted. If structural breakdown occurs, the two curves do not coincide, creating a hysteresis loop. The area enclosed by the loop indicates that degree of breakdown. The major disadvantage of this method is that the investigator arbitrarily sets up the time of shearing and the maximum shear rate (Mewis, 1979). Thus, comparison of data from different investigations becomes difficult.

D. VISCOELASTICITY

The term "viscoelastic" means the simultaneous existence of viscous and elastic properties in a material (Barnes *et al.,* 1989). Some food materials (i.e., food gels) have a unique configuration that will return to the original structure after releasing the deforming stresses. However, the viscous resistance to deformation makes itself felt by delaying the response of the material to a change in stress. The mechanical assemblies called Maxwell and Kelvin models illustrate this point (Fig. 5). These one-dimensional mechanical models consist of springs and dashpots arranged, in parallel

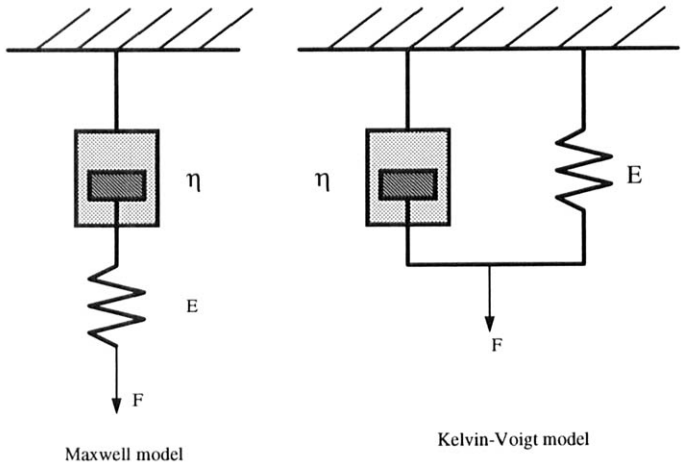

FIG. 5. Schematic diagram of Maxwell and Kelvin–Voigt models.

or in series so that the overall system behaves analogously to a real material, although elements themselves may have no direct analogues in the actual material. The correspondence between the behavior of a model and a real material can be achieved if the differential equation relating force, extension, and time for the model is the same as that relating stress, strain, and time for the material. However, due to the complex composition (i.e., foods contain numerous compounds) and structure of food materials, the use of models such as the Maxwell and the Kelvin–Voigt model and their combination is valid only when the experimental data are obtained within the linear viscoelastic range.

Linear viscoelasticity is the simplest viscoelastic behavior in which the ratio of stress to strain is a function of time alone and not of the strain or stress magnitude. Under a sufficiently small strain, the molecular structure will be practically unaffected, and linear viscoelastic behavior will be observed. At this sufficiently small strain (within the linear range), a general equation that describes all types of linear viscoelastic behavior can be developed by using the Boltzmann superposition principle (Dealy and Wissbrun, 1990). For a sufficiently small strain (γ_0) in the experiment, the relaxation modulus is given by

$$\tau(t)/\gamma_0 = G(t). \tag{7}$$

Consider a sequence of small shear strains as shown in Fig. 6. The shear stress resulting from the strain that occurs at time t_1 will be

$$\tau(t) = G(t - t_1)\delta\gamma(t_1). \tag{8}$$

Assuming the incremental response of the material to this second step strain is independent of the strain introduced at time t_1, the stress resulting from the strain at time t_2 can be simply added on as

$$\tau(t) = G(t - t_1)\delta\gamma(t_1) + G(t - t_2)\delta\gamma(t_2). \tag{9}$$

For any combination of N small strains, the contributions to the stress can continue to be added on, and, in general

$$\tau(t) = \sum_{i=1}^{N} G(t - t_i)\delta\gamma(t_i) \qquad (t > t_N). \tag{10}$$

For a smooth strain history not consisting of finite steps, the following expression can be obtained by use of the definition of the integral

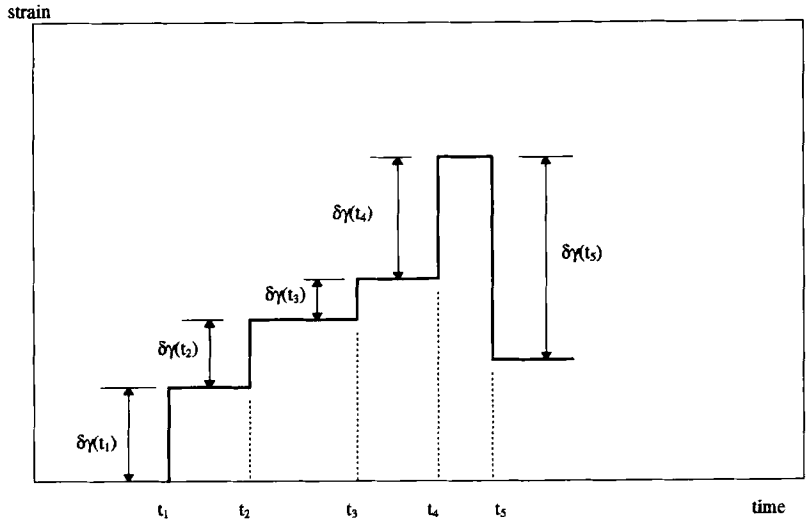

FIG. 6. The diagram of a sequence of step strains. The resulted stress can be superposed if all strain is within the linear viscoelastic range [see Eqs. (8–10); after Dealy and Wissbrun, 1990].

$$\tau(t) = \int_{-\infty}^{t} G(t - t')\mathrm{d}\gamma(t'). \tag{11}$$

Noting that the strain that occurs during the time interval dt' is simply $\dot{\gamma}(t')dt'$, this can also be written as

$$\tau(t) = \int_{-\infty}^{t} G(t - t')\dot{\gamma}(t')dt'. \tag{12}$$

The use of the lower limit of minus infinity is a mathematical convenience; it implies that to calculate the stress at time t, in the most general case, one must know the strain history infinitely far into the past, i.e., at all times t' prior to time t. In practice this is not necessary. In general, an experiment is started at some time ($t = 0$) when the material is in a stress-free state. In this case, $\tau(0) = 0$, and

$$\tau(t) = \int_{0}^{t} G(t - t')\mathrm{d}\gamma(t'). \tag{13}$$

The above equations only apply to shearing deformations, but they can be generalized for any type of deformation by using another feature of linear viscoelasticity. The relaxation process is independent not only of the

magnitude of the strain, but also of the type (kinematics) of the deformation. Thus, the shear strain can be replaced by the strain tensor for infinitesimal strain, and the shear stress can be replaced by the stress tensor to obtain the following alternative form of the Boltzmann superposition principle

$$\tau_{ij}(t) = \int_{-\infty}^{t} G(t - t')\mathrm{d}\gamma_{ij}(t'). \tag{14}$$

$$\tau_{ij}(t) = \int_{-\infty}^{t} G(t - t')\dot{\gamma}_{ij}(t')dt'. \tag{15}$$

Using the Boltzmann superposition principle, it is possible to calculate the stress components resulting from any types of deformation, as long as the deformations are sufficiently small or slow so that linear behavior is exhibited.

III. EXPERIMENTAL METHODS

The rheological concepts such as viscosity, elasticity, and viscoelasticity have just been reviewed. To determine the material functions by carefully defined experimental methods is important in food rheology. In general, two types of tests have been used to characterize rheological properties of food materials: fundamental and empirical tests. Empirical tests have been developed from practical experience as a rapid way to measure something that is related to textural quality. These tests are usually arbitrary, poorly defined, have no absolute standard, and are effective for only a limited number of foods (Bourne, 1994). In contrast, fundamental tests are conducted on a given material by imposing a well-defined stress and measuring the resulting strain or strain rate or by imposing a well-defined strain or strain rate and by measuring the stress developed. The simple shear flow and extensional flow are most common approaches in the fundamental rheological tests (Bird *et al.*, 1987). In this section various tests such as steady shear measurements, extensional flows, and linear viscoelasticity used to characterize the rheological properties of food materials are introduced. The mathematical constraints and simplifications associated with the experimental methods for rheological measurements are discussed.

A. STEADY SHEAR MEASUREMENT

Consider the flow shown in Fig. 1, where a fluid between two plates is sheared as the top plate moves with velocity V_x in the x direction. The

velocity gradient or shear rate is given by $\dot{\gamma}_{xy} = -dV_x/dy = \dot{\gamma}$, and macroscopically is given by V_x/δ, where δ is the plate separation. The stresses generated by the flow act both parallel to the direction of shear (i.e., shear stress) and perpendicular to the direction of shear (normal stress P_{yy} in Fig. 7). The experimentally observable stress perpendicular to the direction of flow includes the stresses arising from fluid motion and the isotropic hydrostatic pressure. It is customary to eliminate the isotropic pressure by taking the difference between normal stresses. The material functions for steady shear flow are defined as

(1) viscosity

$$\eta = -\tau_{yx}/\dot{\gamma}_{yx} \tag{16}$$

(2) primary normal stress coefficient

$$\psi_1 = -\frac{P_{xx} - P_{yy}}{\dot{\gamma}_{yx}^2} \tag{17}$$

(3) secondary normal stress coefficient

$$\psi_2 = -\frac{P_{yy} - P_{zz}}{\dot{\gamma}_{yx}^2}, \tag{18}$$

where τ_{yx} $(= P_{yx})$ is shear stress (Pa), $P_{xx} - P_{yy}$ $(= N_1)$ is primary normal

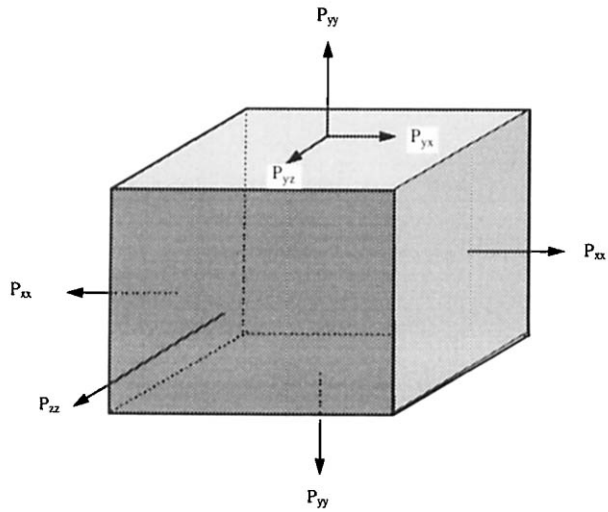

FIG. 7. Force components acting on a cube shaped volume element.

stress difference (Pa), and $P_{yy} - P_{zz}$ $(= N_2)$ is secondary normal stress difference (Pa).

For a Newtonian fluid, the apparent viscosity η is a constant, and the normal stress differences N_1 and N_2 are zero for all. For non-Newtonian fluids, these material functions vary with shear rate.

B. EXTENSIONAL FLOW

The extensional flow is a deformation that involves stretching along streamlines. According to the resulting deformation, it can be classified as uniaxial, biaxial, or planar extension.

1. Uniaxial Extension

The uniaxial extension is illustrated in Fig. 8. If the x_1 axis is aligned with the principal stretching direction, it can be noted that two fluid particles located on this axis will get further apart as the deformation proceeds. It is convenient to use a coordinate system in which the axes are oriented in the directions of the principal strain axes. For this choice, the strain rate components always have the general form

$$\dot{\gamma}_{ij} = \begin{bmatrix} a_1 & 0 & 0 \\ 0 & a_2 & 0 \\ 0 & 0 & a_3 \end{bmatrix}, \tag{19}$$

where a_1, a_2, a_3 have units of reciprocal time and $a_1 + a_2 + a_3 = 0$ for an incompressible material.

The uniaxial extensional flow, with regard to describing both the deformation and the resulting stresses, is uniform shear free flow, in which the strain rate is the same for every material element, and there is no relative

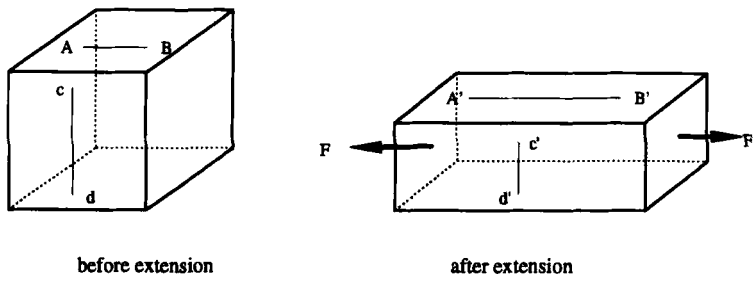

FIG. 8. Effect of simple extension on an initially cubical fluid element.

rotation of perpendicular axes fixed in a fluid element. It is convenient to use the principal strain directions as the coordinate axes, and, in this case, the rate of strain tensor has only diagonal components, as shown in Eq. (19). The shear free flow that has been most used in experimental rheology is uniaxial extension, also called simple extension, which is an axisymmetric flow with stretching in the direction of the axis of symmetry. The effect of uniaxial extension on the shape of an initially cubic fluid element is sketched in Fig. 8.

In the simple extension, the velocity distribution is given by

$$v_1 = \dot{\varepsilon} x_1 \tag{20a}$$

$$v_2 = -\frac{1}{2}\dot{\varepsilon} x_2 \tag{20b}$$

$$v_3 = -\frac{1}{2}\dot{\varepsilon} x_3, \tag{20c}$$

since the flow is axisymmetric, it can also be conveniently described using cylindrical coordinates

$$v_z = \dot{\varepsilon} z \tag{21a}$$

$$v_r = -\frac{1}{2}\dot{\varepsilon} r \tag{21b}$$

$$v_\theta = 0, \tag{21c}$$

where $\dot{\varepsilon}$, the Hencky strain rate, is defined as

$$\dot{\varepsilon} = \frac{d\varepsilon}{dt} = \frac{1}{\mathrm{L}}\frac{dL}{dt} = \frac{d(\ln L)}{dt}. \tag{22}$$

The components of the rate of deformation tensor are given as

$$\dot{\gamma}_{ij} = \begin{bmatrix} 2\dot{\varepsilon} & 0 & 0 \\ 0 & -\dot{\varepsilon} & 0 \\ 0 & 0 & -\dot{\varepsilon} \end{bmatrix}. \tag{23}$$

It is also noted that the principal stresses for extensional flow are in the same direction as those for the strain rate. Thus, the stress tensor also has only diagonal components

$$\sigma_{ij} = \begin{bmatrix} \sigma_{11} & 0 & 0 \\ 0 & \sigma_{22} & 0 \\ 0 & 0 & \sigma_{33} \end{bmatrix}. \tag{24}$$

For incompressible fluids, only the differences between normal stress components have a rheological significance, and the "net tensile stress," in uniaxial extension, is defined as

$$\sigma_E \equiv \sigma_{11} - \sigma_{22} = \sigma_{11} - \sigma_{33}. \tag{25}$$

If $\dot{\varepsilon}$ is independent of time, the flow is steady simple extension, and since this is a motion with constant stretch history, it should be associated with a material function in which times does not appear as an independent variable. For an axially symmetric flow, the stress is also symmetric with

$$\sigma_{22} = \sigma_{33} = \sigma_{rr}. \tag{26}$$

Thus, there is one independent normal stress difference, and a material function having the units of viscosity can be defined as

$$\eta_T(\dot{\varepsilon}) \equiv \frac{\sigma_{11} - \sigma_{22}}{\dot{\varepsilon}} = \frac{\sigma_{zz} - \sigma_{rr}}{\dot{\varepsilon}}. \tag{27}$$

This property is called the "extensional viscosity."

2. *Biaxial Extension*

Another axisymmetric extensional flow is biaxial extension. In this deformation, there is a compression along the axis of symmetry that stretches in the radial direction, as shown in Fig. 9. The principal strain rate is defined as

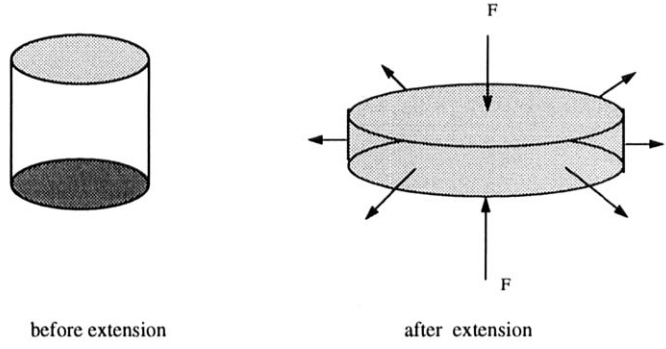

FIG. 9. Biaxial extension.

$$\dot{\varepsilon}_b \equiv v_r/r. \tag{28}$$

For a circular disk having a radius R, this "biaxial strain rate" would be

$$\dot{\varepsilon}_b = \frac{1}{R}\frac{dR}{dt} = \frac{d(\ln R)}{dt}. \tag{29}$$

Furthermore, when this flow is looked upon as biaxial stretching, it is thought of as being generated by a radial, tensile stress rather than an axial, compressive stress. Thus, the "biaxial extensional viscosity" is defined as

$$\eta_b \equiv \frac{\tau_{rr} - \tau_{zz}}{\dot{\varepsilon}_b}. \tag{30}$$

C. TRANSIENT FLOW

One of the characteristics of the viscoelastic foods is that when a shear rate is suddenly imposed on them, the shear stress displays an overshoot and eventually reaches a steady state value. Campanella and Peleg (1987c), Kokini and Dickie (1981), and Dickie and Kokini (1982) presented stress overshoot data for different foods. Figure 10 illustrates stress overshoot as a function of shear rate.

The stress overshoot data can be modeled by means of an equation which contains rheological parameters related to the stress (normal and shear) and shear rate. One such equation is that of Leider and Bird (1974)

$$\sigma_{12} = -K(\dot{\gamma})^n[1 + (b\dot{\gamma}t - 1)e^{(-t/an\lambda)}], \tag{31}$$

where σ_{12} is the shear stress, K and n are power law parameters relating the shear stress and the shear rate, $\dot{\gamma}$ is the imposed sudden shear rate, t is the time, λ is a time constant, and a and b are adjustable parameters.

A number of models have been developed to describe transient viscoelastic behavior and one must have at hand carefully obtained rheological data in order to test the applicability of the models. Another example of the applicability of models to viscoelastic data is the study of Leppard and Christiansen (1975) in which the models proposed by Bogue and Chen, Carreau, and Spriggs were evaluated. In the case of foods, the empirical models have been developed to describe the transient data on stick butter, tub margarine (Mason *et al.*, 1982), canned frosting (Kokini and Dickie, 1981; Dickie and Kokini, 1982), and mayonnaise (Campanella and Peleg, 1987c).

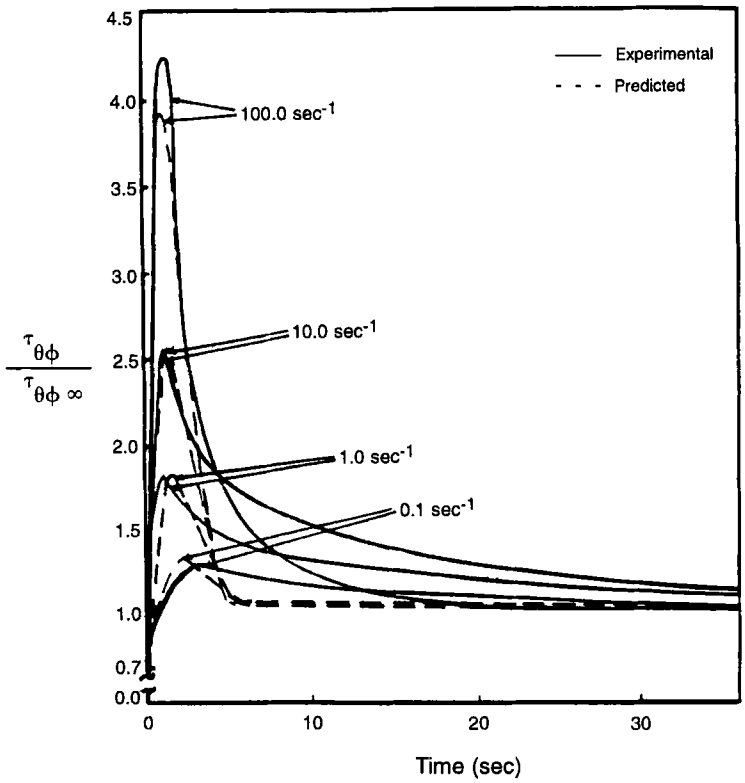

FIG. 10. Shear stress development for peanut butter at 25°C and comparison of the prediction of the Bird–Leider equation with experimental data (Kokini, 1992).

D. LINEAR VISCOELASTICITY

For a number of viscoelastic materials, a linear viscoelastic response can be achieved experimentally if the deforming stresses are kept sufficiently small such that recovery occurs upon unloading. There are a number of tests which may be used to study viscoelastic materials to determine the relationships between stress, strain, and time for a given type of deformation and a given type of loading pattern. The most important tests include creep compliance and recovery test, stress relaxation, and the dynamic oscillatory test. As shown in the thin slab shown in Fig. 1, different deformation patterns can be applied on the upper plate. Assume that the slab is so thin that inertial effects can be ignored and the slab can be regarded as homogeneously deformed with the amount of shear $\gamma(t)$ variable in time. Let $\tau(t)$ be the shearing stress, the force per unit area on the slab. The

following three simple shearing motions illustrate the three experimental methods of stress relaxation, creep compliance, and sinusoidal shear deformation.

1. *Stress Relaxation Test*

When the slab is subject to a single-step shear history $\gamma(t) = \gamma_0 H(t)$, where $H(t)$ is the Heaviside unit step function, zero for negative t and unit for t zero or positive, the stress response can be used to characterize the rheological properties. When the materials are subjected to a step strain as shown in Fig. 11a, the different stress responses are obtained as shown in Fig. 11b. If the material were perfectly elastic, the corresponding stress history would be of the form $\tau(t) = \tau_0 H(t)$, constant for t positive (curve a in Fig. 11b). If the material were an ideal viscous fluid, the stress would be instantaneously infinite during the step and then zero for all positive t, like a Dirac delta, $\delta(t) = H'(t)$ (curve b in Fig. 11b). For most real materials, like semisolid foods, the stress response shows that neither of these idealizations is quite accurate. The stress usually decreases from its initial value

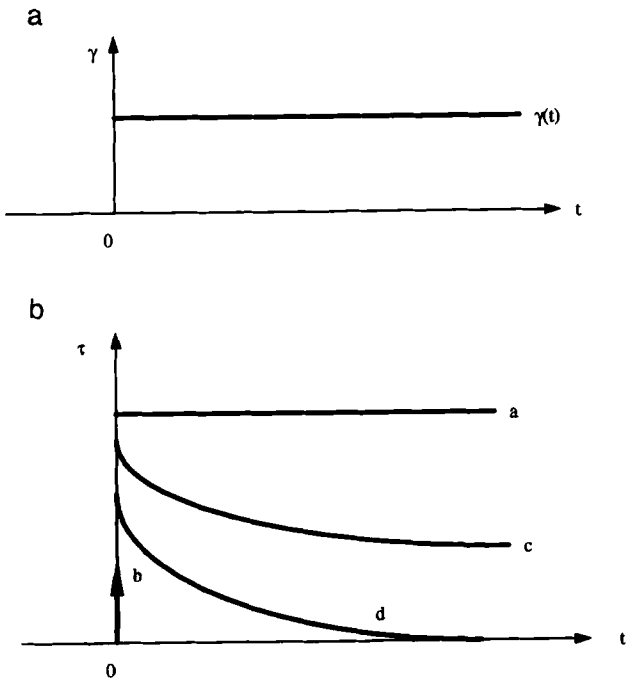

FIG. 11. Stress relaxation of different types of materials in response to the shear strain.

quite rapidly at first and later more gradually, as it approaches some limiting value $\tau(\infty)$. The limiting value is a subjective matter since no one can wait that long, but it is a convenient idea. If the limiting value is not zero, it is likely to call the material a solid (curve c in Fig. 11b), and if the limiting value approaches zero rapidly, the material is then called a fluid (curve d in Fig. 11b).

2. *Creep Test*

Supposing the upper slab subjected to a one-step stress history is $\tau(t) = \tau_0 H(t)$ (Fig. 12a), the response of strain can be used to characterize the creep/recovery behavior of food materials. The creep/recovery response may be classified into several different categories as shown in Figs. 12b to 12e. For a perfectly elastic solid, compliance rises instantaneously to the equilibrium value. When the stress is released, there is an instantaneous recovery (Fig. 12b). All the energy is stored in the solid and there is no energy dissipation. For a viscous fluid, flow occurs in response to the applied stress. As a result, the compliance increases linearly with time with a slope of $1/\eta$, where η is the viscosity. The input energy is totally dissipated due to the motion of the liquid and there is no energy stored. When the stress is released, the compliance does not decrease (since there is no energy release), but stays constant at the final value (Fig. 12c).

The response of viscoelastic materials lies between these two extremes. When a constant stress is applied, there is an instantaneous rise in compliance. The compliance then increases with time to the equilibrium value. When the stress is released, there is an instantaneous drop in the compliance followed by a time-dependent decrease. For a viscoelastic "solid," all the energy is stored, and hence there is a total energy release upon removal of the shear stress. As a result, the final equilibrium compliance is zero (Fig. 12d). For a viscoelastic "liquid," however, viscoelastic flow takes place and there is only a partial recovery when the stress is removed (Fig. 12e).

3. *Sinusoidal Oscillatory Shearing*

The properties of viscoelastic materials can also be described in terms of the responses to sinusoidal inputs. In a sinusoidal shear test, the applied strain or stress to the sample is sinusoidal and, in general, the response of the stress or strain is dependent on both shear frequency and the rate of shear strain (Fig. 13).

A convenient means of manipulating oscillatory quantities is in terms of their complex equivalents, which is based upon the Euler identity

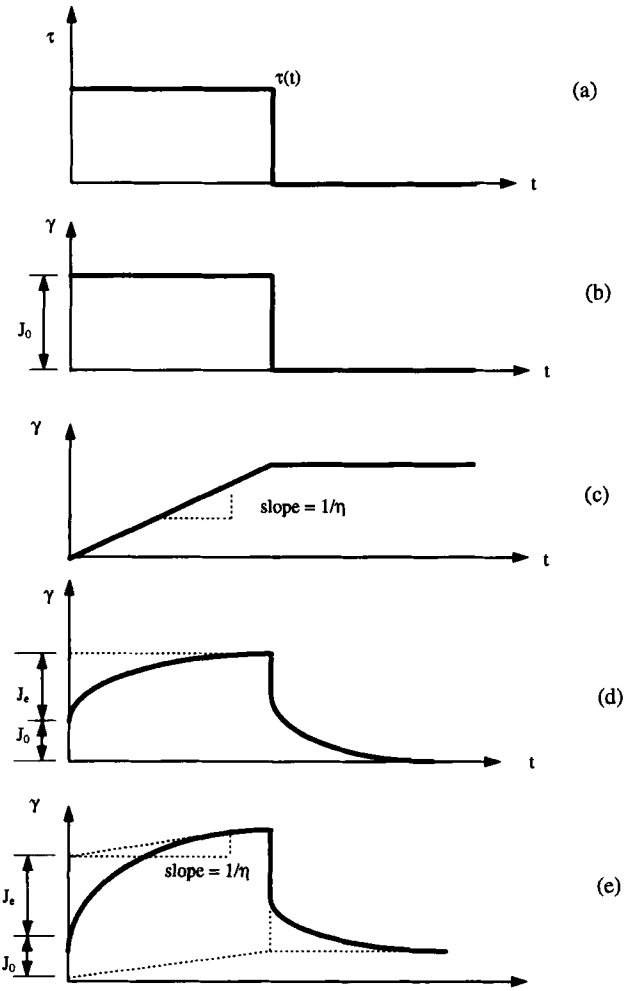

FIG. 12. Creep recovery response of different types of material to the shear stress.

$$e^{i\theta} = \cos(\theta) + i\sin(\theta), \tag{32}$$

where $i = \sqrt{-1}$ (imaginary).

Hence, oscillatory shear strain and stress become

$$\gamma(\omega t) = \gamma_0 e^{i\omega t} \tag{33}$$

$$\tau(\omega t) = \tau_0 e^{i(\omega t+\delta)}, \tag{34}$$

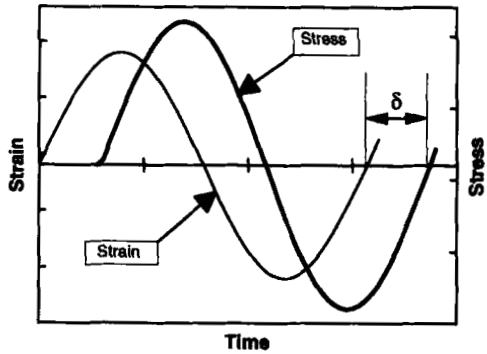

FIG. 13. Small amplitude oscillatory test.

where $\gamma(\omega t)$ is the oscillatory strain input in terms of complex notation, γ_0 is the amplitude of strain, ω is the shear frequency, $\tau(\omega t)$ is the stress output in terms of complex notation, τ_0 is the amplitude of stress, and δ is the phase angle between strain and stress.

During oscillation, the complex shear modulus, G^*, is defined as the ratio of oscillatory stress to oscillatory strain

$$G^* = \frac{\tau(\omega t)}{\gamma(\omega t)}. \tag{35}$$

Substituting Eqs. (33) and (34) into Eq. (35), one obtains

$$G^* = \frac{\tau_0 e^{i(\omega t+\delta)}}{\gamma_0 e^{i\omega t}} = \frac{\tau_0}{\gamma_0} e^{i\delta} = \frac{\tau_0}{\gamma_0}[\cos(\delta) + i \sin(\delta)]. \tag{36}$$

It is customary to write the complex modulus G^* in terms of real and imaginary parts

$$G^* = G' + iG''. \tag{37}$$

Combining Eqs. (36) and (37), one obtains

$$G' = \tau_0/\gamma_0 \cos(\delta) \tag{38}$$

$$G'' = \tau_0/\gamma_0 \sin(\delta). \tag{39}$$

The "in-phase" component, G', represents the elastic character of the material and hence is called the storage modulus (since elastic energy is stored

and can be recovered). The "out-of-phase" component, G'', represents the viscous character and is called the loss modulus (since the viscous energy is dissipated or lost). The tangent of the phase angle δ is sometimes called the loss tangent, since

$$\tan(\delta) = G''/G'. \tag{40}$$

In the linear viscoelastic range, various other material functions relate to one another (Ferry, 1980)

$$\eta' = G''/\omega \tag{41}$$

$$\eta'' = G'/\omega \tag{42}$$

$$\eta^* = \eta' - i\eta'', \tag{43}$$

where η' is the dynamic viscosity, η'' is the out-of-phase component of the complex viscosity, and η^* is the complex viscosity.

Normal stress is an "extra" stress which is developed in viscoelastic material under shear, in directions normal to the plane of shear. The normal stress is expressed by the first and second normal stress coefficients (Bird *et al.*, 1987)

$$\psi_1(\dot{\gamma}) = -\frac{\tau_{11} - \tau_{22}}{\dot{\gamma}^2} \tag{44}$$

$$\psi_2(\dot{\gamma}) = -\frac{\tau_{22} - \tau_{33}}{\dot{\gamma}^2} \tag{45}$$

where $\psi_1(\dot{\gamma})$ is the first normal stress coefficient, and $\psi_2(\dot{\gamma})$ is the second normal stress coefficient.

IV. INSTRUMENTATION IN FUNDAMENTAL RHEOLOGY

The above-discussed material functions (η, G', G'', E', E'', η', η'', $\tan(\delta)$, etc.) are important concepts to characterize the flow and viscoelastic properties of food materials. Furthermore, a rheometer or relevant instrument is an essential tool to determine and evaluate these material functions. One of the most important components of the rheometer is the measuring geometry, because it provides a particular way in deforming the tested material.

The common configurations of measuring geometries are capillary, cone–plate, plate–plate, and concentric cylinder. The following is a review of working equations associated with each geometry and its limitations.

A. CAPILLARY TUBE GEOMETRY

When a fluid is pumped through a certain length of tube, a pressure drop is observed due to the viscous drag effect of the fluid. This pressure drop is a function of the geometric size of the tube (inner diameter and length of tube) and the flow rate. Thus, this relationship is used to determine the viscosity of a fluid. Figure 14 shows a schematic diagram of a capillary tube.

For Newtonian fluids, the viscosity, shear rate, and shear stress at the wall can be determined by the following relationships (Bird *et al.*, 1960; Sherman, 1970)

$$\eta = \frac{\pi \Delta P R^4}{8LQ} \tag{46}$$

$$\tau_R = \frac{\Delta P R}{2L} \tag{47}$$

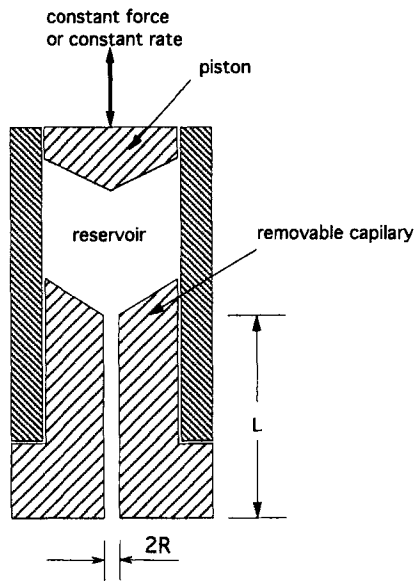

FIG. 14. Schematic diagram of a capillary geometry (Bird *et al.*, 1987).

$$\dot{\gamma}(R) = \frac{4Q}{\pi R^3} \tag{48}$$

where R is the radius of the capillary, Q is the flow rate, L is the length of the capillary, and ΔP is the pressure difference between the two ends of the capillary.

For non-Newtonian fluids, the working equations are modified as follows (Barnes *et al.*, 1989)

$$\dot{\gamma}_R = \frac{4Q}{\pi R^3}\left[\frac{3}{4} + \frac{1}{4}\frac{d(\ln Q)}{d(\ln \tau_w)}\right]. \tag{49}$$

The apparent viscosity for non-Newtonian fluids can then be obtained by combining Eqs. (47) and (49)

$$\eta_a = \frac{\tau_w}{\dot{\gamma}_R} = \frac{\pi R^4 \Delta P}{8QL}\Big/\left[\frac{3}{4} + \frac{1}{4}\frac{d(\ln Q)}{d(\ln \tau_w)}\right], \tag{50}$$

where η_a is the apparent viscosity.

When a non-Newtonian fluid in a capillary tube is subjected to a small amplitude oscillatory pressure gradient, the viscoelastic properties of the fluid can be determined (Darby, 1976). The explicit equations for determining such material functions as η' and η'' are fairly complicated. Equations (51) and (52) are the implicit expressions

$$\eta' = \frac{1}{8}\pi R^4 R(\omega) \tag{51}$$

$$\eta'' = \frac{1}{8}\pi R^4 X(\omega), \tag{52}$$

where R is the radius of the capillary, $R(\omega)$ and $X(\omega)$ are the solutions of the following governing differential equations [Eqs. (53–55)] and boundary conditions [Eq. (56)]

$$\Phi(\omega t) = \frac{\partial P}{\partial z} = \Phi_0 e^{i\omega t} \tag{53}$$

$$\rho\frac{\partial V_z}{\partial t} = -\frac{\partial P}{\partial z} + \frac{1}{r}\frac{\partial}{\partial r}(r\tau_{rz}) \tag{54}$$

$$\tau(\omega t,z) = \eta^*(i\omega)\dot{\gamma}(\omega t,z), \tag{55}$$

$$\begin{Bmatrix} V_z = 0 & \text{at} & r = R \\ dV_z/dt = 0 & & r = 0 \end{Bmatrix}, \tag{56}$$

where $\Phi(\omega t)$ is the oscillatory pressure input with complex argument, $\dot{\gamma}$ is the strain rate, and η^* is the complex viscosity.

However, the above equations [Eqs. (46–56)] are only valid under certain assumptions. These assumptions include:

(1) the fluid is incompressible;
(2) the fluid velocity is zero at the wall (no slippage at the wall);
(3) the normal stress is isotropic; and
(4) a unique function of $\dot{\gamma} = f(\tau)$ relates the rate of shear ($\dot{\gamma}$) to shear stress (τ).

Not all of these assumptions are met by a capillary rheometer. In the capillary geometry, the source of errors can be: (1) entrance (end) effects; (2) kinetic energy imparted to a sample; (3) wall effect; (4) turbulent flow; and (5) plug flow (Sherman, 1970). The entrance effect in capillary flow is due to an abrupt change in the velocity profile and shear distribution when the material is forced from a large diameter reservoir into the capillary tube. However, this effect can be eliminated by using a long entrance region and determining the pressure drop as the difference of two pressure values measured in the fully developed laminar flow region (Kokini, 1992).

It is assumed that there is no slip at the boundaries in derivation of equations to calculate shear rates from capillary and rotational viscometer data. However, many foods form a thin layer of liquid at solid boundaries and this in turn results in deviation from the no-slip boundary condition. The errors due to slippage at walls were studied by Kokini and Plutchok (1987a) in capillary viscometers and by Higgs (1974) in capillary and concentric cylinder viscometers in accordance with the pioneering theoretical study of Mooney (1931).

In the capillary viscometer, the slip phenomena can also be observed due to inhomogenous flow (Cohen and Metzner, 1986; de Vargas *et al.*, 1993). Therefore, the influence of the slip phenomenon must be considered when analyzing the data. In the case of 0.2% xanthan gum solution, the slip velocity is an increasing function of the wall shear stress and also of the length to diameter ratio *L/D*. However, the slip velocity becomes independent of *L/D* at large *L/D* (de Vargas *et al.*, 1993).

B. CONE–PLATE GEOMETRY

Cone–plate geometry consists of a flat plate and a rotating cone forming a very small angle with the plate (Fig. 15a). The angle (θ_0) between the cone and plate is usually between 0.5° and 3°. The food material to be tested is sheared between the rotating cone and the fixed plate. The following expressions are used to determine the steady shear rheological parameters (Bird *et al.*, 1960, 1987)

$$\eta(\dot{\gamma}) = \frac{3T\theta_0}{2\pi R^3\dot{\gamma}} \tag{57}$$

$$\dot{\gamma} = \frac{\Omega}{\sin(\theta_0)} \tag{58}$$

$$\tau = \frac{3T}{2\pi R^3 \sin^2\left(\frac{\pi}{2} - \theta_0\right)} \tag{59}$$

$$\psi_1(\dot{\gamma}) = \frac{2F}{\pi R^2\dot{\gamma}^2} \tag{60}$$

$$\psi_1(\dot{\gamma}) + 2\psi_2(\dot{\gamma}) = -\frac{1}{\dot{\gamma}^2} \cdot \frac{\partial \pi_{\theta\theta}}{\partial \ln(\dot{\gamma})} \tag{61}$$

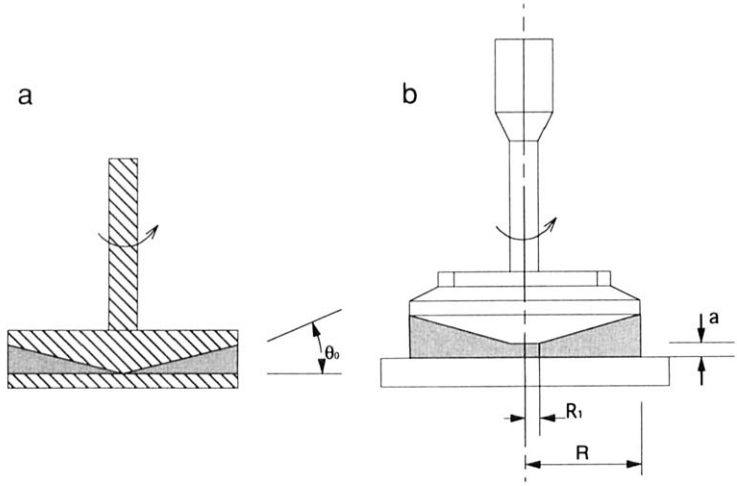

FIG. 15. Schematic diagram of cone–plate geometry.

where R is the radius of the plate, θ_0 is the angle between the cone and plate, Ω is the angular velocity of the cone, T is the measured torque, F is the force required to keep the tip of the cone in contact with the circular plate, $\pi_{\theta\theta}$ is the measured pressure by a flush-mounted pressure transducer located on the plate, ψ_1 is the first normal stress coefficient, and ψ_2 is the second normal stress coefficient.

Since θ_0 is very small (ca. 0.5–3°, or 0.0087–0.0523 radians), $\sin^2(\pi/2 - \theta_0)$ will close to one, and τ will be nearly independent of position [see Eq. (59)]; that is, the tested material between the gap will experience uniform shear stress. This is the advantage of cone–plate compared to other geometries (i.e., capillary tube and parallel disk). For example, at an angle of 1°, the percentage difference in shear stress between cone and plate is 0.1218% (Fredrickson, 1964). This is within the precision of measurements that must be made; therefore, one can assume that shear stress, and, hence, shear rate and apparent viscosity, are uniform throughout the fluid.

When the upper cone oscillates within a small deformation, the viscoelastic properties are calculated by the following governing equations (Bird *et al.*, 1987)

$$\eta' = \frac{3\theta_0 T_0 \sin(\delta)}{2\pi R^3 \omega \gamma_0} \tag{62}$$

$$\eta'' = \frac{3\theta_0 T_0 \cos(\delta)}{2\pi R^3 \omega \gamma_0}, \tag{63}$$

where γ_0 is the deformation, T_0 is the amplitude of the oscillating torque, δ is the phase angle, ω is the oscillating shear frequency, θ_0 is the angle between cone and plate (usually less than 4^0), and R is the radius of the cone. Using the relationships in Eqs. (41–43), the other linear viscoelastic material functions, such as G', G'', and $\tan(\delta)$, can be obtained.

In practice, the cone is often truncated by a small amount which avoids contact with the cone tip (which might become worn) and the plate (which might become indented). Figure 15b shows the schematic diagram of a truncated cone–plate geometry. A truncated cone also facilitates tests on suspensions (Barnes *et al.*, 1989). If $R_1 < 0.2R$, the torque is reduced by less than 1%. The total torque is reduced by much less than 1% because the parallel plate section near the axis will contribute to the torque (Whorlow, 1980).

For cone–plate geometry, the major errors are the edge and end effects which arise from the fact that the geometry has finite dimensions and a fracturing effect (Walters, 1975).

C. PLATE–PLATE GEOMETRY

The plate–plate geometry consists of two disks (Fig. 16). The food material to be tested is placed between two parallel plates. During the measurement, one plate is stationary while the other is rotating or oscillating, depending on the measuring mode. Compared to cone–plate geometry, plate–plate geometry has the advantage of a flexible gap which allows for a wider measuring range and more applications. The disadvantage is that the distribution of shear stress in the test material is not uniform.

In rotational mode, the following expressions can be used to determine the apparent viscosity and the normal stress from the measurement of the torque on the fixed bottom plate (Bird *et al.*, 1987)

$$\dot{\gamma}_R = \frac{\Omega R}{H} \tag{64}$$

$$\eta(\dot{\gamma}_R) = \frac{T}{2\pi R^3 \dot{\gamma}_R}\left[3 + \frac{d(\ln(T/2\pi R^3))}{d(\ln\dot{\gamma}_R)}\right] \tag{65}$$

$$\psi_1(\dot{\gamma}_R) - \psi_2(\dot{\gamma}_R) = \frac{F/\pi R^2}{\dot{\gamma}_R}\left[2 + \frac{d(\ln(F/\pi R^2))}{d(\ln\dot{\gamma}_R)}\right] \tag{66}$$

$$\psi_2(\dot{\gamma}_R) = \frac{P_a - \Pi_{zz}(R)}{\dot{\gamma}_R^2}, \tag{67}$$

where R is the radius of the plate, H is the separation of the plates, Ω is

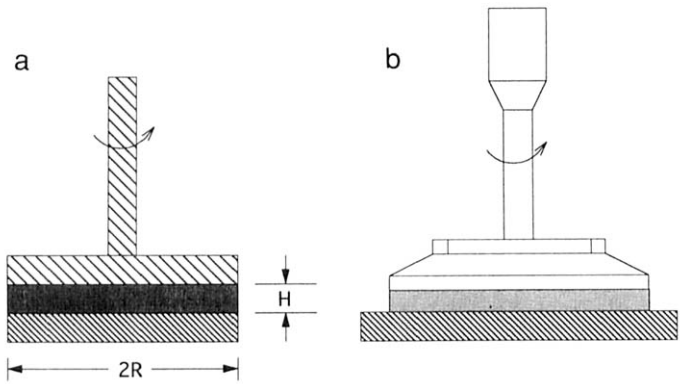

FIG. 16. Schematic diagram of plate–plate geometry.

the angular velocity of the upper plate, ψ_1 and ψ_2 are the first and second normal stress coefficients, respectively, T is the torque required to rotate the upper plate, $\dot{\gamma}_R$ is the shear rate at the edge of the plate, F is the force required to keep the separation of the two plates constant, P_a is the atmospheric pressure, and $\Pi_{zz}(R)$ is the normal pressure measured on the disk at the rim.

When the upper plate oscillates sinusoidally with frequency ω and angular amplitude γ_0 ($\gamma_0 \ll 1$), the time-dependent torque (T) is measured. The following expression is used to determine η' and η'' from the measurements with $\gamma_0 \ll 1$ (Bird *et al.*, 1987)

$$\eta' = \frac{2HT_0 \sin(\delta)}{\pi R^4 \omega \gamma_0} \tag{68}$$

$$\eta'' = \frac{2HT_0 \cos(\delta)}{\pi R^4 \omega \gamma_0}, \tag{69}$$

where T and γ_0 are the measured torque and angular amplitude, respectively. The phase angle, δ, is the measured phase shift ($0 \leq \delta \leq \pi/2$).

The limitation of plate–plate geometry is that the shear rate has to be below 500 sec^{-1} (Connelly and Greener, 1985). The major sources of error associated with the plate–plate viscometer may be surface fracture, radial migration, and wall slippage. The advantage of plate–plate geometry is that it provides flexibility for the material such as coarse dispersions, which are intolerant of the narrow gaps associated with either cone–plate or concentric cylinder rheometers. The plate separation provides a simple means to extend the shear rate range and to test for sample slip (Shoemaker *et al.*, 1987; Yoshimura and Prud'homme, 1988).

Specimen slippage has been previously reported. Navickas and Bagley (1983) detected slip between gels formed by wheat starch granules and the parallel plates of a Rheometrics Model KMS-71 mechanical spectrometer. Slippage has also been detected in the measurement of flowability of molten cheese by capillary rheology (Konstance and Holsinger, 1992), in the measurement of apple sauce by concentric cylinder rheometer (Qiu and Rao, 1989, 1990), and in the measurement of mayonnaise with parallel plates of a Physica rheometer (Ma and Barbosa-Cánovas, 1995a).

Several methods have been employed to overcome the slippage problem during rheological measurement. One is to use a cyanoacrylate ester adhesive to attach the gel to the plates (Konstance and Holsinger, 1992).

Another approach to prevent slippage is to use an upper plate with 80-μm teeth (Rosenberg *et al.*, 1995).

D. CONCENTRIC CYLINDER GEOMETRY

The basic features of concentric cylinder geometry are shown in Fig. 17. Depending on whether the inner cylinder or outer cylinder rotates, the concentric cylinder geometry is referred to as Couette or Searle type. In a Searle type (Fig. 17a), the inner cylinder rotates, while in a Couette type (Fig. 17b), the outer cylinder rotates. For both types, the fluid to be tested is sheared in the gap between the cylinders. The torque necessary to maintain the position of the fixed cylinder is a measure of the shear stress after certain corrections have been made, and the rotational speed of the moving cylinder is the measure of the rate of shear. Equations (70) through (72) represent the working equations for both types of concentric cylinder geometry (Couette and Searle type) with the assumptions: (1) steady laminar, isothermal flow; and, (2) negligible gravity and end effect.

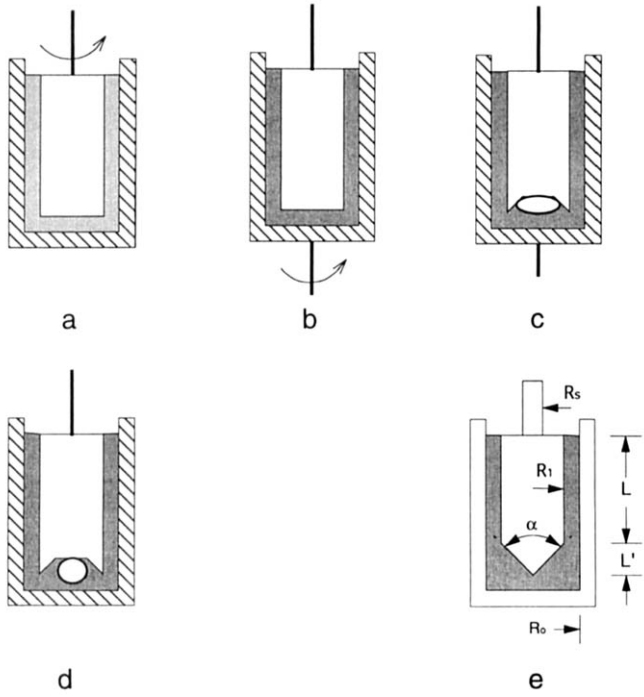

FIG. 17. Schematic diagram of concentric cylinder geometry.

$$\tau = \frac{T}{2\pi L R_i^2} \tag{70}$$

$$\dot{\gamma}(R_i) \cong \dot{\gamma}(R_o) = \frac{2\Omega}{1 - \kappa^2}. \tag{71}$$

The viscosity of Newtonian fluid is given by Margules' equation:

$$\eta = \frac{T}{4\pi L\Omega}\left(\frac{1}{R_i^2} - \frac{1}{R_o^2}\right), \tag{72}$$

where L is the length of the bob, R_i is the radius of the bob, R_o is the radius of the cup, T is the torque, and κ is defined as the ratio of the radius of the cup to the radius of the bob (R_i/R_o).

If the gap is very small compared to the radius of the cylinder, there is little variation in the shear rate across the gap. Therefore, the shear rate can be approximated by the simplified equation

$$\dot{\gamma} \approx \frac{\Omega R_i}{R_O - R_i}. \tag{73}$$

When the outer cylinder undergoes a very small sinusoidal oscillation in a tangential direction, this motion causes the inner cylinder, suspended by a torsion wire, to oscillate with the same frequency but with different amplitude and phase. The viscoelastic properties of the fluid can be determined by the expressions (Bird *et al.*, 1987)

$$\eta' = \frac{-\rho BWA\sin(\delta)}{1 + A^2 - 2A\cos(\delta)} \tag{74}$$

$$\eta'' = \frac{\rho BWA[A - \cos(\delta)]}{1 + A^2 - 2A\cos(\delta)}, \tag{75}$$

where ρ is the density, W, A and δ are all functions of the dimensionless frequency $\tilde{\omega}$, and B is the instrument parameter defined by

$$B = (a - 1)^2 R^2(\sqrt{K/I}), \tag{76}$$

where K is the torsion constant of the wire and I is the moment of inertia for the bob.

The major sources of errors associated with concentric cylinders are the end effects and turbulent flow in the end region. Princen (1986) proposed a modification to eliminate the end effects in a concentric cylinder rheometer. He proposed adding a pool of mercury at the bottom of the cup that essentially eliminates the torque exerted on the bottom of the inner cylinder and on the sample in the gap. However, the limitation of this modification is that the fluid to be tested must be considerably more viscous than mercury, and the angular velocity of the cup must be kept below the levels where centrifugal force or normal force effects start to significantly alter the shape of the sample/air and sample/mercury interfaces.

Another feature of some commercial rheometers is a well in the bottom of the inner cylinder in order to minimize the end effect (Fig. 17c). Its purpose is to trap an air bubble and thus eliminate the torque on the bottom. However, it has been demonstrated that the bubble immediately balls up and assumes the shape of a sessile bubble, so that a major fraction of the bottom area is again in contact with the field (Fig. 17d). Alternatively, the shape of the end of the cylinder can be chosen as a cone (see Fig. 17e) (angle equal to $\tan^{-1}[(R_o - R_i) / R_o]$) such that the shear rate in the liquid trapped between the cone and the bottom is the same as that in the liquid between the cylinders.

V. CONSTITUTIVE MODELS

Rheological studies become particularly useful when predictive relationships between rheological properties and the responsible structural unit of food materials are being developed. However, most food materials have a complex structure and composition (i.e., foods contain numerous compounds) which makes modeling very difficult. In order to understand the relationship between rheological properties and the structures of food materials, idealization of their conformations is necessary. A typical example is the freely jointed chain consisting of springs and beads (Bird *et al.*, 1987). This idealization leads to models which describe stresses developed in materials as a result of an applied deformation. The models which are able to describe the relationship between components of stress and strain as well as strain rate are referred to as constitutive equations (Bird *et al.*, 1987; Bagley, 1992a; Darby, 1976).

A. RHEOLOGICAL MODEL FOR STEADY SHEAR FLOW

The simplest rheological equation of state is for the Newtonian fluid where viscosity is the only material property needed to characterize the

fluid flow (Prud'homme, 1991). For a non-Newtonian fluid, the Newtonian model may be generalized by allowing the viscosity to be a function of shear rate, leading to the generalized Newtonian fluid model (Prud'homme, 1991). The power law (Eq. 3b) and the Herschel–Bulkley equation (Eq. 4) are examples of a generalized Newtonian fluid model. Another popular model is the Casson model which has the expression

$$\tau^{1/2} = (\tau_0)^{1/2} + K(\dot{\gamma})^{1/2}, \tag{77}$$

where τ is the shear stress, τ_0 is the yield stress, K is the consistency index, and $\dot{\gamma}$ is the shear rate.

The power law, Herschel–Bulkley equation, and Casson model are simple and easy to use. However, these equations only work for modeling steady shear flows rather than transient or elongational flows. Thus, many other models have been proposed to fit experimental data more closely for food materials. Among these, it is worth mentioning the Ree–Eyring equation which has three constants

$$\eta = \eta_\infty + (\eta_0 - \eta_\infty) \cdot [\text{Arcsin}h(\beta\dot{\gamma})] / (\beta\dot{\gamma}), \tag{78}$$

where β is a molecular relaxation time, and η_0 and η_∞ are limiting viscosity at zero shear rate ($\dot{\gamma} \to 0$) and at a very large shear rate ($\dot{\gamma} \to \infty$), respectively. This equation has been used by Doublier and Launay (1976, 1981) for guar gum and locust bean gum solutions with satisfactory results. However, when the shear rate range was extended up to or near the first Newtonian zone (a very low shear rate region ($\dot{\gamma} \to 0$) where the apparent viscosity is independent of shear rate), the model fit was not as close (Launay and Pasquet, 1982).

One equation, initially developed by Cross (1965) for dispersed systems, has given good fits to the experimental flow curve for several polysaccharide solutions and dispersions over a very large shear range, extending, in a few cases, from the first to second Newtonian zones [the zones where the apparent viscosity is independent of shear rate at a very low shear rate region ($\dot{\gamma} \to 0$) and a very large shear rate region ($\dot{\gamma} \to \infty$), respectively]

$$\eta = \eta_\infty + (\eta_0 - \eta_\infty) / [1 + (t \cdot \dot{\gamma})^m], \tag{79}$$

where t is a relaxation time and m is a nondimensional exponent. When both $\eta \ll \eta_0$ and $\eta \gg \eta_\infty$, Eq. (79) predicts a power behavior where $(1 - m)$ approaches the flow index (n).

Doublier and Launay (1981) have calculated the four parameters of the Cross equation for guar gum by a computerized nonlinear regression

method, but no physical meaning was assigned to η_∞ because it was extrapolated outside the measurement range. The mean relative deviations (MRD) between calculated and measured viscosities were typically 1–3%, but the Newtonian viscosity, η_0, was not reached experimentally.

B. DILUTE SOLUTION MOLECULAR THEORIES

Dilute solution molecular theories are beginning to find applications in food polymer rheology. Chou *et al.* (1991) tested the Rouse (1953) and Zimm (1956) theories for random coils and the Marvin and McKinney (1965) theory for rod-like molecules in reference to citrus pectin solutions. In the Rouse concept, the molecules are totally free draining without considering hydrodynamic interactions. In the Zimm approximation, on the other hand, it is assumed that hydrodynamic interactions have a significant effect and are taken into account when calculating the spectrum of relaxation times. At the other extreme, it is possible to develop molecular models which approximate the flow behavior of elongated molecules as rigid rods. Examples include Yamakawa's cylinder, the Shishkebab model, and Ullmann's cylinder (Ferry, 1980). Marvin and McKinney (1965) also developed a model approximating rod-like behavior, but when Kokini and Chou (1993) compared the dilute solution behavior of apple pectin with the Zimm, Rouse, and rod-like theories, the Zimm model gave the best approximation.

The equations to predict the reduced moduli and relaxation time of flexible random coil molecules of Rouse and Zimm types are

$$[G']_R = \sum_{p=1}^{n} \frac{\omega^2 \tau_p^2}{(1 + \omega^2 \tau_p^2)} \tag{80}$$

and

$$[G'']_R = \sum_{p=1}^{n} \frac{\omega \tau_p}{(1 + \omega^2 \tau_p^2)}, \tag{81}$$

where ω is the frequency, τ_p is the spectrum of relaxation time, $[G']_R$ is the reduced storage modulus, and $[G'']_R$ is the reduced loss modulus.

The reduced storage modulus, reduced loss modulus, and relaxation time spectrum are given by

$$\lim_{c \to 0} [G']_R = \frac{G' M}{cRT} \tag{82}$$

$$\lim_{c \to 0} [G'']_R = \frac{(G'' - \omega\eta_s)M}{cRT} \tag{83}$$

$$\tau_p = \frac{K_p[\eta]\eta_s M}{cRT}, \tag{84}$$

where G' and G'' are the storage modulus and loss modulus of the dilute solution, respectively, M is the molecular weight, c is the concentration, R is the ideal gas constant, T is the absolute temperature, and η_s is the solvent viscosity.

To predict rigid rod behavior several theories are available. The general form of these predictions are

$$[G']_R = \frac{m_1\omega^2\tau^2}{(1 + \omega^2\tau^2)} \tag{85}$$

$$[G'']_R = \omega\tau\left[\frac{m_1}{1 + \omega^2\tau^2} + m_2\right] \tag{86}$$

and

$$\tau = \frac{m[\eta]\eta_s M}{RT} \tag{87}$$

and m is given by

$$m = (m_1 + m_2)^{-1}, \tag{88}$$

where m_1 and m_2 are empirical constants.

Table II shows the values of these constants for five different rigid rod models. The predicted reduced moduli from the theory of Marvin and

TABLE II

EMPIRICAL CONSTANTS m_1 AND m_2 FOR THE ELONGATED RIGID ROD MODEL[a]

Model	m_1	m_2	m
Cylinder (Yamakawa, 1975)	0.60	0.29	1.15
Cylinder (Ullman, 1969)	0.46	0.16	1.61
Rigid dumbbell (Marvin and McKinney, 1965)	0.60	0.40	1.00
Prolate ellipsoid (Cerf, 1952)	0.60	0.24	1.19
Shishkebab (Kirkwood and Auer, 1951)	0.60	0.20	1.05

[a]Source: Kokini, 1993.

McKinney (1965) for rigid dumbbells as a function of $\omega\tau$ are given in Fig. 18, and the predicted moduli for random coil theories of Rouse and Zimm are shown in Fig. 19. At high frequencies, the reduced moduli of the Rouse theory become equal and increase together with a slope of 1/2, while those in the Zimm theory remain unequal and increase in a parallel manner with a slope of 2/3.

C. CONCENTRATED SOLUTION/MELT THEORIES

1. The Bird–Carreau Model

The Bird–Carreau model is an integral model which involves taking an integral over the entire deformation history of the material (Bistany and Kokini, 1983). This model can describe non-Newtonian viscosity, shear rate-dependent normal stresses, frequency-dependent complex viscosity, stress relaxation after large deformation shear flow, recoil, and hysteresis loops (Bird and Carreau, 1968). The model parameters are determined by a nonlinear least squares method in fitting four material functions (α_1, α_2, λ_1, and λ_2).

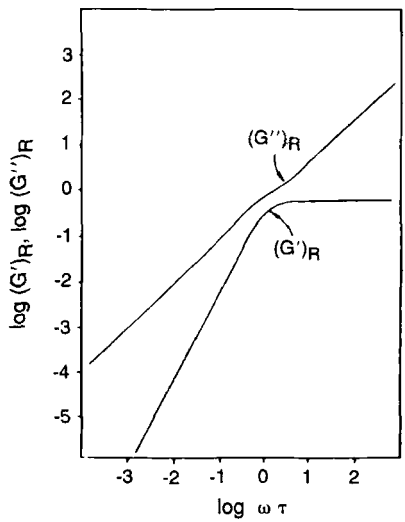

FIG. 18. Predictions of reduced moduli for the rigid rod theory of Marvin and McKinney (1965).

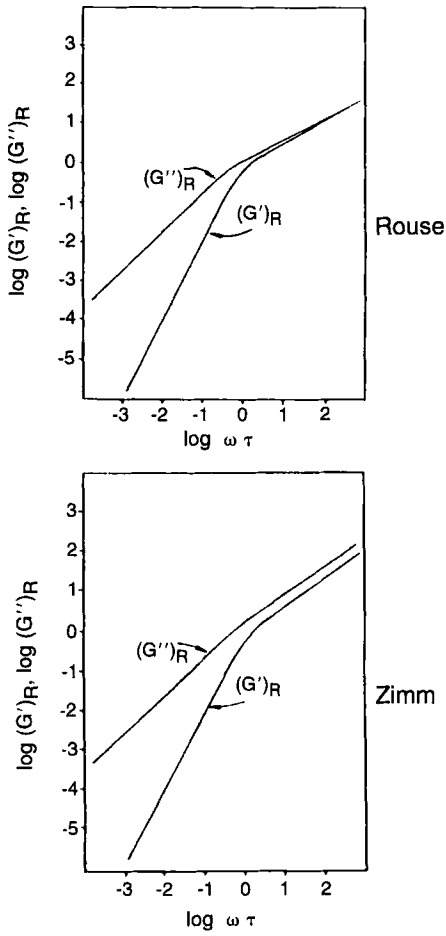

FIG. 19. Prediction of reduced moduli for flexible random coils as proposed by Rouse (1953) and Zimm (1956).

The Bird–Carreau model (Bird and Carreau, 1968; Carreau *et al.*, 1968) prediction for η is

$$\eta = \sum_{p=1}^{\infty} \frac{\eta_p}{1 + (\lambda_{1p}\dot{\gamma})^2} \tag{89}$$

and at larger shear rates, the above equation is approximated by

$$\eta = \frac{\pi\eta_o}{Z(\alpha_1) - 1} \cdot \frac{(2^{\alpha_1}\lambda_1\dot{\gamma})^{(1-\alpha_1)/\alpha_1}}{2\alpha_1 \sin[(1 + \alpha_1)\pi/2\alpha_1]}, \tag{90}$$

where $\lambda_{1p} = \lambda_1[2/(p + 1)]^{\alpha_1}$
$\eta_p = \eta_o\lambda_{1p}/\Sigma\eta_{1p}$
$Z(\alpha_1) = \Sigma\ k^{-\alpha_1}$.

The Bird–Carreau prediction for η' is

$$\eta' = \sum_{p=1}^{\infty} \frac{\eta_p}{1 + (\lambda_{2p}\omega)^2} \tag{91}$$

and, at high frequencies, η' is approximated by

$$\eta' = \frac{\pi\eta_o}{Z(\alpha_1) - 1} \cdot \frac{(2\alpha_2\lambda_2\omega)^{(1-\alpha_1)/\alpha_2}}{2\alpha_2 \sin\left(\frac{1 + 2\alpha_2 - \alpha_1}{2\alpha_2} \cdot \pi\right)}. \tag{92}$$

Finally, the prediction for η''/ω is

$$\eta''/\omega = \sum_{p=1}^{\infty} \eta_p \cdot \frac{\lambda_{2p}}{1 + (\lambda_2 p\omega)^2}, \tag{93}$$

which converges to the following equation at high frequencies

$$\eta''/\omega = \frac{2^{\alpha 2}\lambda_2\pi\eta_o}{Z(\alpha_1) - 1} \cdot \frac{(2^{\alpha_2}\lambda_2\omega)^{(1-\alpha_1-\alpha_2)/\alpha_2}}{2\alpha_2 \sin\left(\frac{1 + \alpha_2 - \alpha_1}{2\alpha_2} \cdot \pi\right)}, \tag{94}$$

where $\lambda_{2p} = \lambda_2\ (2/p + 1)^{\alpha 2}$.

The Bird–Carreau model employs the use of four empirical constants (α_1, α_2, λ_1, and λ_2) and a zero shear limiting viscosity (η_0) of the solutions. The constants α_1, α_2, λ_1, and λ_2, can be obtained by two different methods: one method is using a computer program which can combine least square method and the method of steepest descent analysis for determining parameters for the nonlinear mathematical models (Carreau *et al.*, 1968). Another way is to estimate by a graphic method as illustrated in Fig. 20: two constants, α_1 and λ_1, are obtained from a logarithmic plot of η vs $\dot{\gamma}$, and the other two constants, α_2 and λ_2, are obtained from a logarithmic plot of η' vs ω.

2. *Doi and Edwards Theory*

A molecular theory of viscoelasticity of molten, high molecular weight polymers that makes use of the reptation concept has been developed by

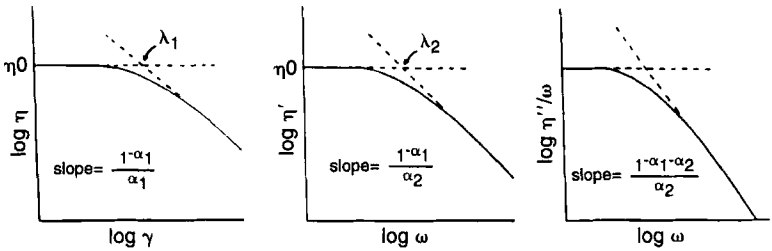

FIG. 20. Determination of the Bird–Carreau constants λ_1, λ_2, α_1, α_2 (from Bird *et al.*, 1977).

Doi and Edwards (1978, 1979, 1986). They started with the Rouse-segmented chain model for a polymer molecule. Because of the presence of neighboring molecules, there are many places along the chain where lateral motion is restricted, as shown in Fig. 21. To simplify the representation of these restrictions, Doi and Edwards assume that they are equivalent to placing the molecule of interest in the "tube" as shown in Fig. 22. This tube has a diameter d and length L. The mean field is represented by a three-dimensional cage. The primitive chain can move randomly forward or backward only along itself. For a monodisperse polymer, the linear viscoelasticity is characterized by

$$G'(\omega) = \frac{8}{\pi^2} G_N^0 \sum_{p\text{odd}} \frac{(\omega T_1)^2/p^6}{1 + (\omega T_1)^2/p^4} \tag{95}$$

$$G''(\omega) = \frac{8}{\pi^2} G_N^0 \sum_{p\text{odd}} \frac{(\omega T_1)/p^6}{1 + (\omega T_1)^2/p^4} . \tag{96}$$

FIG. 21. Sketch showing one entire molecule together with the segments of other molecules that are located near to it and restrict its motion (from Dealy and Wissbrun, 1990).

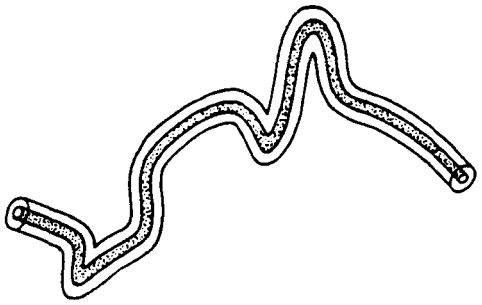

FIG. 22. Sketch showing the hypothetical tube assumed by Doi and Edwards to be equivalent in its effect to the segments shown in Fig. 21 (from Dealy and Wissbrun, 1990).

T_1 is given by

$$T_1 = \frac{\pi^2 \eta_0}{8 G_N^0 \sum 1/p^4}, \tag{97}$$

where G_N^0 is the terminal region plateau modulus, ω is the frequency of the applied shear field, and p is the normal mode of motion. The lower limit of summation for p is 1. The upper limit is estimated from the viscosity versus concentration plot as

$$p(\text{upper limit}) = \frac{\phi_c}{\phi_e}, \tag{98}$$

where ϕ_e is the volume fraction of polymer in a solution and ϕ_c is the volume fraction of polymer in solution at the critical concentration.

For a polydisperse system the theory has been modified by Rahalkar *et al.* (1985) with the results

$$G'(\omega) = G_N^0 \int_0^\infty \frac{8}{\pi^2} \sum_{p\text{odd}} \frac{(\omega T_1)^2 \mu^6 f(\mu)/p^6}{1 + (\omega T_1)^2 \mu^6/p^4} \, d\mu \tag{99}$$

$$G''(\omega) = G_N^0 \int_0^\infty \frac{8}{\pi^2} \sum_{p\text{odd}} \frac{(\omega T_1) \mu^3 f(\mu)/p^4}{1 + (\omega T_1)^2 \mu^6/p^4} \, d\mu, \tag{100}$$

where μ is dimensionless molecular weight, and $f(\mu)$ is normalized molecular weight distribution.

D. SOLID FOODS

Some foods exist in the form of a gel, so it is useful to determine the mechanism of gelation in new product development. Oakenfull and Scott

(1988) demonstrated that for weak gels, information about the junction zone—the regions of polymer where the molecules interact to form a gel network—can be derived from the kinetics of gelation and from the relationship between shear modulus and concentration. The equations to predict the junction zone (n) are

$$G = \frac{(RTc/M) \cdot (M[J] - c)}{M_J - c} \tag{101}$$

and

$$K_J = [J]M_J^n \cdot [n(c - M_J[J])]^{-n}, \tag{102}$$

where M is the number average molecular weight of the polymer, M_J is the number average molecular weight of the junction zone, $[J]$ is effectively the molar concentration of the junction zone, n is the number of cross-linking loci that form a junction zone, c is the concentration of the gum solution, K_J is an association constant, R is the gas constant (1.987 cal · g/(mol · ^{0}K), and T is the temperature (^{0}K).

Combining Eqs. (101) and (102) to eliminate the quantity $[J]$, a relationship between shear modulus (G) and concentrations (c) in terms of M, M_J, K_J, and n can be obtained using numerical methods. The best fit experimental data of G versus c, the number of polysaccharide chains involved in a junction zone (n), as well as information about the size and the thermodynamic stability of junction, can also be obtained. Table III shows the results obtained by Oakenfull and Scott (1988) after applying Eqs. (101) and (102). The data in Tabel III indicate that kappa-carrageenan has a larger junction zone (M_J) than iota-carrageenan by a factor of more than two; kappa-carrageenan's junction zones are also thermodynamically more stable with

TABLE III

SIZE AND THERMOSTABILITY OF THE JUNCTION ZONE IN GELS OF KAPPA-CARRAGEENAN CALCULATED FROM SHEAR MODULUS DATA AT 298°K

	Kappa-carrageenan	Iota-carrageenan
M	10,500	17,800
M_J	8,900	4,100
n	6.4	2.1
K_J	1.65×10^{23}	554
ΔG_J°	−133	−15.6
No. of monomers units per junction zone	37	14
ΔG_J° per monomer	−3.58	−1.12

a free energy of formation (ΔG_J) of −133 kJ/mol for kappa-carrageenan compared to −15.6 kJ/mol for iota-carrageenan. Thus, iota-carrageenan forms softer, weaker gels than kappa-carrageenan at equivalent concentrations.

Ainsworth and Blanshard (1980) demonstrated that the creep curves of gels could be described by a Maxwell element in series with one or more Voigt elements as described by the equation

$$J(t) = J_o + \sum_i J_i \cdot (1 - e^{-t/\tau_i}) + t/\eta_N, \tag{103}$$

where $J(t)$ is the measured compliance, J_o and J_i are the compliance of the Maxwell and Voigt springs, respectively, η_N is the viscosity of the Maxwell dashpot, and τ_i is the retardation time associated with the Voigt element.

A modified Maxwell model and a nonexponential model were used by Nussinovitch *et al.* (1989) for characterization of the stress relaxation of agar and alginate gels as described by the equation

$$\frac{F(t)}{F_O} = 1 - \frac{t}{k_1 + k_2 t} \tag{104}$$

or in its linear form

$$\frac{F_0 \cdot t}{F_o - F(t)} = k_1 + k_2 t, \tag{105}$$

where F_0 is the initial force, $F(t)$ is the decaying force, and k_1 and k_2 are the constants.

The force–time relationship in relaxation was fit to Eq. (105) using linear regression to yield the constants k_1 and k_2. The same relationship normalized and fit using nonlinear regression is described by the modified Maxwell model

$$\frac{F(t)}{F_o} = C_o + C_1 \cdot \exp\left[-\left(\frac{t}{10}\right)\right] + C_2 \cdot \exp\left[-\left(\frac{t}{100}\right)\right]. \tag{106}$$

Equations (105) and (106) are two different mathematical models for characterizing the relaxing behavior of agar and alginate gels. The main advantage of Eq. (105) is that it is a simple mathematical form which has the possibility of calculating its constant by simple linear regression. The model expressed by Eq. (106) is mathematically more elaborate, and it provides a more detailed account of the shape of the relaxation curves of

gels. This detail, however, comes at the expense of having to use a nonlinear regression procedure to determine its coefficients (Nussinovitch *et al.*, 1989).

VI. APPLICATIONS OF RHEOLOGY IN CHARACTERIZING ENGINEERING PROPERTIES OF FOODS

A. STEADY SHEAR VISCOSITY OF FLUID FOODS AND DILUTE FOOD POLYMER SOLUTIONS

The steady shear flow properties of fluid foods, including most beverages such as tea, coffee, beer, wines, and soda pop, and biopolymer materials, such as carbohydrates and protein, can be used in engineering design. Simple liquids, true solutions, low molecular weight solvents, dilute macromolecule dispersions in low molecular weight solvents, and noninteracting polymer solutions exhibit Newtonian behavior. Sugar solutions also exhibit these flow characteristics. Several researchers have studied the viscosity of sucrose solutions because they are often used to calibrate viscometers (Muller, 1973; see Table IV).

Milk, which is an aqueous emulsion of butter fat globules of 1.5–10 μm in diameter and contains about 87% water, 4% fat, 5% sugar (mainly lactose), and 3% protein (mainly casein), is a Newtonian liquid. Fernández-Martín (1972) pointed out that the viscosity of milk depends on temperature, concentration, and the physical state of fat and proteins which in turn is affected by thermal and mechanical treatments. Fernández-Martín (1972)

TABLE IV

COEFFICIENT OF VISCOSITY OF SUCROSE SOLUTIONS AT 20°C (MULLER, 1973)

Sucrose (%)	g/100 g water	Viscosity (mPa · sec)
20	25.0	2.0
25	33.2	2.5
30	42.9	3.2
35	53.8	4.4
40	66.7	6.2
45	81.8	9.5
50	100.0	15.5
55	122.2	28.3
60	150.0	58.9
65	185.7	148.9
70	233.3	485.0
75	300.0	2344.0

found that unconcentrated milks were Newtonian liquids, but concentrated milk showed a weak dependence on shear.

All oils have a fairly high viscosity because of their long chain molecular structure. The longer the chain of the fatty acids, the higher the viscosity. Polymerized oils have a much higher viscosity than nonpolymerized oils. The viscosity of an oil also increases with saturation of the carbon double bonds. At a temperature higher than melting point, the artificial fat demonstrates a Newtonian behavior in the experimental shear range, but the viscosity is greatly dependent on its composition (Drake *et al.*, 1994; see Table V). Generally, it appears that the greater the molecular interaction, the greater the viscosity. Table V demonstrates the dependency of viscosity of oil on the fatty acid composition, temperature, and its substitutes.

Some fruit juices also exhibit Newtonian flow, such as filtered apple juice up to 30° Brix, Concord grape juice up to 50° Brix, and filtered orange juice of 10 and 18° Brix (Saravacos, 1970). This behavior is found in the 20–70°C temperature range. Depectinated and clarified fruit juices (apple, peach, pear, etc.) also exhibit Newtonian behavior (Rao *et al.*, 1984;

TABLE V

VISCOSITY OF SELECTED OIL AND ARTIFICIAL OIL

Name	Temperature (°C)	Viscosity (Pa · sec)	References
Corn oil	25	0.0565	Steffe *et al.* (1986)
	38	0.0317	
Olive oil	10	0.138	Steffe *et al.* (1986)
	40	0.0363	
	70	0.0124	
Rapeseed oil	0	2.53	Steffe *et al.* (1986)
	20	0.16	
	30	0.096	
Soybean oil	30	0.046	Steffe *et al.* (1986)
	50	0.0206	
	90	0.0078	
Mfat[a]	50	0.016	Drake *et al.* (1994)
M SPE[b]	50	0.272	Drake *et al.* (1994)
MM SPE[c]	50	0.215	Drake *et al.* (1994)
MC SPE[d]	50	0.200	Drake *et al.* (1994)
MT SPE[e]	50	0.104	Drake *et al.* (1994)

[a]Mfat, anhydrous milkfat.
[b]M SPE, milkfat sources polyester.
[c]MM SPE, milkfat : myristate sources polyester.
[d]MC SPE, milkfat : coconut sources polyester.
[e]MT SPE, milkfat : tallow sources polyester.

Ibarz *et al.*, 1987, 1989, 1992). Other important foods that show Newtonian behavior are table syrups such as honey, corn syrup, blends of sucrose, and molasses. Examples of the rheological properties of several foods were listed by Barbosa-Cánovas and Peleg (1983), Barbosa-Cánovas *et al.* (1993), Steffe (1992b), and Kokini (1992).

However, most fluid foods exhibit a non-Newtonian behavior instead of the Newtonian behavior discussed above. Thus, the power law equation (Eq. 3), Herschel–Bulkley equation (Eq. 4), and the Casson equation (Eq. 77) are often used in characterizing flow properties of food. The parameters of these models for some foods are shown in Table VI. One has to keep in mind that the power law equation, Herschel–Bulkley equation, and Casson equation are often valid for about two or three logarithmic cycles of shear rate, and the range of shear rate tested should always be recorded to prevent erroneous results from extrapolation outside this range. For a wider shear rate range, the Ree–Eyring equation or Cross equation [Eqs. (78) and (79)] needs to be used. Table VII shows the application of the Ree–Eyring equation for orange juice at different temperatures (Vitali and Rao, 1984). It is noted that food products such as apple sauce, mustard, and tomato ketchup are time dependent, since the parameters calculating from the first shear curve differed from the second shear curve (see Table VI) (Barbosa-Cánovas and Peleg, 1983).

Many semisolid food materials portray yield stress. The yield stress in polysaccharide dispersions results from intermolecular hydrogen bonding and molecular entanglements (Gencer, 1985). A precise quantitative knowledge of yield stress is necessary since it is very important in pumping operations, stability of suspensions, appearance of coated materials, and consumer acceptability (Kee and Durning, 1990).

Yield stresses can be measured with a variety of techniques. These include measuring the shear stress at vanishing shear rates, extrapolation of data using rheological models that include yield stresses and stress relaxation experiments, and others (Barbosa-Cánovas and Peleg, 1983; Lang and Rha, 1981).

Kee and Durning (1990) reviewed two principal methods of measuring yield stresses: dynamic and static methods. One example of the dynamic method is the extrapolation from the flow curve. Equation (4) is often used to determine the yield stress of gum solutions. Table VIII lists the examples of yield stress of several selected food commodities measured from different methods. It is noted that for the same food product, different methods have different yield stress value. In addition to the measuring method, the embedded factor—the composition of food products—also needs to be emphasized. For instance, in mayonnaise, the concentration of oil and xanthan gum significantly affected the yield stress since it increased from

TABLE VI

RHEOLOGICAL PARAMETERS OF SELECTED FOODS

Product	TSS (°Brix)	Flow curve	Power law		Herschel–Bulkley model				Casson model			References
			K	n	τ_0	K	n	SS	τ_0	K	SS	
Apple sauce	18.2	1st			33	31	0.16	49	8.0	0.16	461	Barbosa-Cánovas and Peleg (1983)
(Matt's)		2nd			34	6.8	0.42	42	6.5	0.24	82	
Apple sauce	18.1	1st			26	33	0.15	216	7.8	0.16	705	
(Stop & Shop)		2nd			30	6.4	0.43	116	6.1	0.25	153	
Mustard	—	1st			20	37	0.21	462	7.9	0.26	1196	
(Gulden's)		2nd			35	5.5	0.52	251	6.4	0.34	280	
Mustard	—	1st			17	16	0.29	1244	6.1	0.25	1406	
(Stop & Shop)		2nd			20	3.4	0.56	634	4.8	0.32	641	
Tomato ketchup	23.2	1st			21	9.4	0.38	46	5.8	0.26	133	
(Heinz)		2nd			24	2.2	0.61	36	4.9	0.49	53	
Tomato ketchup	34.4	1st			15	6.4	0.4	43	4.8	0.24	88	
(Stop & Shop)		2nd			15	2.0	0.6	74	4.0	0.27	75	
Orange juice (low pulp)		—										
−18.5°C			29.16	0.712								Rao *et al.* (1984)
−14.1°C			14.58	0.757								
−9.3°C			10.80	0.743								
−5.0°C			7.88	0.721								
−0.7°C	65.0		5.93	0.711								
10.1°C			2.72	0.725								
19.9°C			1.64	0.721								
29.5°C			0.91	0.739								
Concentrated orange juice	65											
(Hamlin, early)					1.32	0.083	0.859					Crandall *et al.* (1982)
(Hamlin, late)					0.94	0.031	1.055					

TABLE VII

REE–EYRING EQUATION PARAMETERS FOR PERANP SAMPLE[a]

Temp (°C)	η_0	β	η_∞	SS[b]
−18.8	76.61	0.2338	65.02	600
−14.5	42.04	0.1211	35.77	1.531
−9.9	27.03	0.1096	23.54	291
−5.4	16.09	0.0747	13.71	433
−0.8	9.98	0.0500	8.37	522
9.5	4.25	0.0259	3.63	571
19.4	2.62	0.0393	2.15	154
29.2	1.69	0.0421	1.41	29

[a]Source: Vitali and Rao, 1984. PERANP was a 65°Brix, 5.7% pulp sample made from Pera oranges.

[b]SS is the sum of the squares of deviation between the data and the model.

23 to 235 Pa as the oil concentration increased from 75 to 85% or from 55 to 195 Pa as the xanthan gum concentration increased from 0.5 to 1.5% (Ma and Barbosa-Cánovas, 1995b).

Yoshimura *et al.* (1987) compared the yield stress of a series of model oil-in-water emulsions determined from three techniques: concentric cylinder, parallel disk, and a vane. The techniques give comparable results, with parallel disk having the largest uncertainty when measuring the yield stress. No one technique is superior to the others but each has advantages and limitations. Experimentally it is easier to change gap spacing on parallel disks with the sample in place than to remove the sample, change cylinders, and reload the concentric cylinder geometry. Experiments using the vane method with a stress rheometer are easy to perform and are of high precision. Viscosity information cannot be obtained since the flow field around the vanes is quite complex after flow begins. The technique requires large volumes of sample relative to the other two methods.

B. CHARACTERIZATION OF ENTANGLEMENT IN CONCENTRATED SOLUTION

Viscoelastic properties of biopolymeric materials such as carbohydrates and protein can be used to characterize their three-dimensional configuration in solutions. This configuration affects their functionality in many food products. An understanding of how the molecular structure of polymers affects their rheological properties can make it possible to predict and improve the flow behavior of newly developed food products that have such

TABLE VIII
YIELD STRESS OF SELECTED FOODS

Products	Yield stress (Pa)	Method	References
Apple sauce	58.6	Stress decay	Charm (1963)
Apple sauce	45–87	Squeezing flow	Campanella and Peleg (1987b)
Apple sauce	46–82		Qiu and Rao (1988)
Ketchup	22.8	Extrapolation	Ofoli *et al.* (1987)
Ketchup	15.4–16.0	Stress to initiate flow	De Kee *et al.* (1980)
Ketchup	18–30	Squeezing flow	Campanella and Peleg (1987b)
Ketchup	26–30	Vane method	Missaire *et al.* (1990)
Mayonnaise	24.8–26.9	Stress to initiate flow	De Kee *et al.* (1980)
Mayonnaise	81–91	Squeezing flow	Campanella and Peleg (1987b)
Mustard	34.0	Extrapolation	Ofoli *et al.* (1987)
Mustard	52–78	Squeezing flow	Campanella and Peleg (1987b)
Tomato puree	23.0	Stress decay	Charm (1963)
Tomato puree	25–34	Vane method	Missaire *et al.* (1990)
Emulsion			Yoshimura *et al.* (1987)
EM1B	120 ± 5	Concentric cylinder	
	100 ± 50	Parallel disks	
	104 ± 2	Vane	
EM2B	240 ± 5	Concentric cylinder	
	270 ± 50	Parallel disks	
	241 ± 2	Vane	
EM3B	460 ± 10	Concentric cylinder	
	450 ± 50	Parallel disks	
	471 ± 4	Vane	
EM2A	570 ± 10	Concentric cylinder	
	460 ± 50	Parallel disks	
	536 ± 4	Vane	
EM2C	42 ± 1	Concentric cylinder	
	80 ± 20	Parallel disks	
	48 ± 2	Vane	

polymers (Liguori, 1985). Examples can be found at the consistency and stability improvement of emulsions by using polymers with enhanced surface activity and greater viscosity and elasticity.

Constitutive equations were applied to simulate viscoelasticity of concentrated food polymer dispersions. Some fundamental and empirical models have been discussed in Section V. Among them, the Bird–Carreau constitutive model [Eqs. (89–94)] have been used for food polymer dispersions (Kokini *et al.*, 1984; Kokini and Plutchok, 1987b; Plutchok and Kokini, 1986).

In Fig. 23, the Bird–Carreau model is compared to the experimental data of a 1.0% guar solution in the frequency/shear rate range of 0.1 to 100 sec^{-1}.

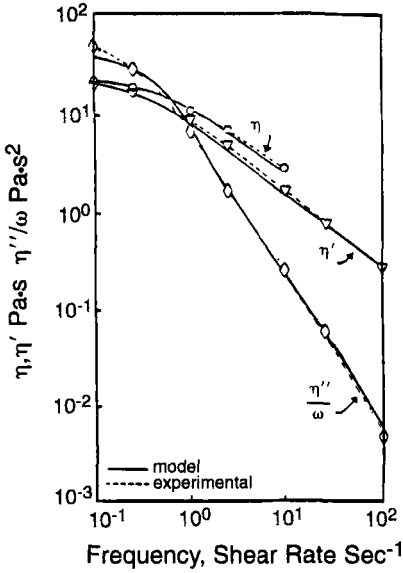

FIG. 23. Comparison of predictions of the Bird–Carreau constitutive model and experimental data for 1% guar solution (Kokini *et al.*, 1984).

For η''/ω, the model very accurately predicted the high-frequency region. The low-frequency region was predicted somewhat less accurately. Experimental values of log η' versus log ω and log η versus log $\dot{\gamma}$ were fit quite accurately by the model.

Such constitutive models can also be used to predict the rheological properties of concentrated gum blend systems as well. Plutchok and Kokini (1986) developed empirical equations capable of predicting η_O, λ_1, and λ_2, as well as the slope of the non-Newtonian region of η and η', using concentration and molecular weight data. The equations to predict rheological constants of CMC, guar gum, and CMC:guar blend ratios of 3:1, 2:1, 1:1, 1:2, and 1:3 in the concentration range of 0.5 to 1.5% by weight are

$$\eta_0 = 1.06 \cdot 10^{19} \cdot c_{\text{blend}}^{3.63} \cdot M_{w,\text{blend}}^{-2.94}$$

$$\lambda_1 = 1.81 \cdot 10^{5} \cdot c_{\text{blend}}^{1.75} \cdot M_{w,\text{blend}}^{-0.92}$$

$$\lambda_2 = 1.63 \cdot 10^{9} \cdot c_{\text{blend}}^{1.72} \cdot M_{w,\text{blend}}^{-1.72}$$

$$S_\eta = 1.63 \cdot 10^7 \cdot c_{\text{blend}}^{0.50} \cdot M_{w,\text{blend}}^{-1.26}$$

$$S_{\eta'} = 2.17 \cdot 10^7 \cdot c_{\text{blend}}^{0.32} \cdot M_{w,\text{blend}}^{-1.26},$$

where $M_W = X_1 M_{W1} + X_2 M_{W2}$; X_i is mass fraction, M_w is weight-average molecular weight (g/g · mol), M_{W1} and M_{W2} are molecular weight of each component of the blend

$$c_{\text{blend}} = v_1 c_1 + v_2 c_2,$$

where v_i is the volume fraction and c_{blend} is the concentration (g/100 ml).

Using these empirical equations in conjunction with the predictions of the Bird–Carreau model, it is possible to predict η' and η''/ω. An example of such a plot is shown in Fig. 24 for a 1.0% CMC:guar blend (3:1). Experimental data are superimposed on these plots to judge the aptness of the model. The steady shear viscosity η and the dynamic viscosity η' are well predicted in the shear rate range of 0.1 to 100 sec^{-1}. The experimental data, as well as the theoretical prediction, portray commonly observed behaviors by polymeric dispersions. In this instance, η and η' for this blend ratio tend to some value, a property suggested by the Bird–Carreau model at low shear rate (Kokini *et al.*, 1984).

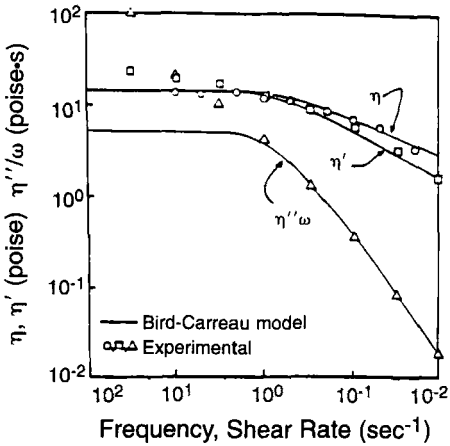

FIG. 24. Comparison of prediction of the Bird–Carreau constitutive model and experimental data for a 3:1 CMC:guar blend at a total concentration of 1% (Kokini, 1993).

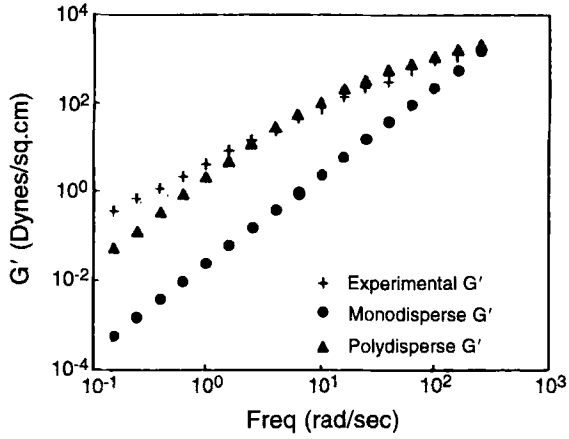

FIG. 25. Predictions of G' values for a 5% pectin solution using the Doi–Edwards model (Kokini, 1993).

To predict G' and G'' values for 5% pectin dispersion the equations assuming a monodisperse polymer as well as the equations assuming a polydisperse polymer were used. For the polydisperse case, a computer program was developed to account for a small molecular fraction measured using low-angle light scattering coupled with HPLC. Figures 25 and 26 show the plot of predicted values along with the experimental values for the simulations of G' and G'', respectively. It is clear that the polydisperse

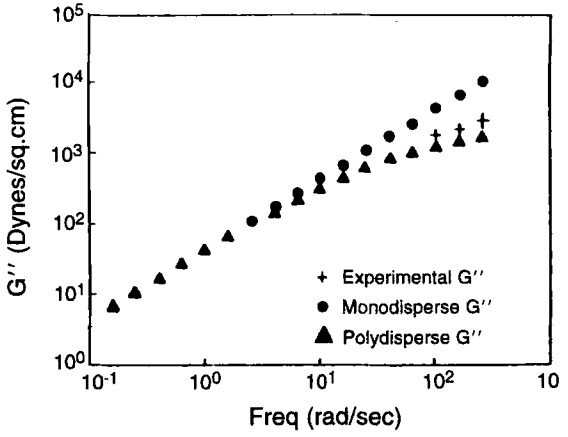

FIG. 26. Predictions of G'' values for a 5% pectin solution using the Doi–Edwards model (Kokini, 1993).

model explains the experimental data much better than the monodisperse model, which is in agreement with the polydispersity ratios ($\overline{M}_W/M_n$) ranging from 15 to 45 (Chou and Kokini, 1987; Shrimanker, 1989).

C. APPLICATION OF CONSTITUTIVE EQUATIONS IN DOUGH RHEOLOGY

The ability to accurately predict the nonlinear viscoelastic behavior of a wheat dough is of practical interest to scientists developing new products or technologies in the food industry. Because of the many different processing schemes in use it is necessary to accurately predict the rheological behavior, especially the steady viscosity and the primary normal stress coefficient, through a shear rate range which is relevant to processing. The Bird–Carreau model, although semiempirical, provides the accuracy and the versatility which should make it of particular interest to those working with wheat dough. Using small amplitude oscillatory properties, Smith *et al.* (1970) showed that as protein content increased in a protein (gluten)–starch–water system the magnitude of both the storage modulus (G') and loss modulus (G'') increased. Hibberd and Wallace (1966) reported a critical strain of approximately 0.5% beyond which wheat dough rheological properties became nonlinear. Dus and Kokini (1990) showed that the steady shear rheological properties (η, N_1) and small amplitude rheological properites (η' and η''/ω) could be successfully simulated using the Bird–Carreau constitutive model.

The experimental and predicted values of the steady viscosity function versus shear rate are given in Figure 27. The experimental data are well

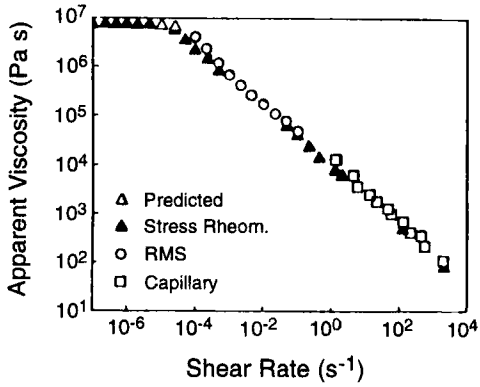

FIG. 27. Experimental values and those predicted using the Bird–Carreau model of apparent viscosity (η) as a function of shear rate for hard flour dough sample (Dus and Kokini, 1990).

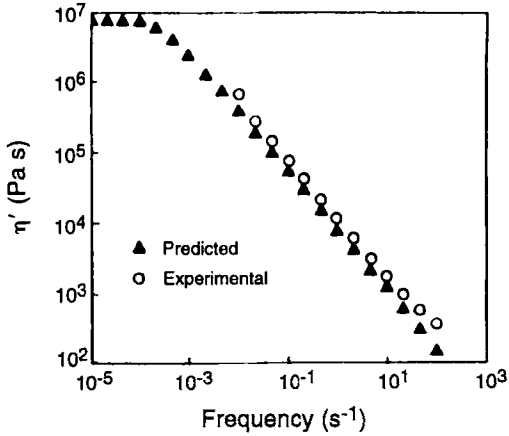

FIG. 28. Experimental and predicted values of dynamic viscosity (η') versus frequency for the 40% moisture hard flour dough sample (Dus and Kokini, 1990).

simulated by the Bird–Carreau model. Comparison of experimental data versus the predicted data shows a high degree of superposition throughout the range of viscosity.

The prediction of η' and the experimental data versus frequency in Fig. 28 show that the prediction works well. This is especially so at the intermediate frequencies where the prediction is very close. The experimental data are seen to deviate slightly at the extremes of the frequency range.

Figure 29 shows the predicted and experimental values of η''/ω versus frequency. In the range of frequencies tested there is a very high degree

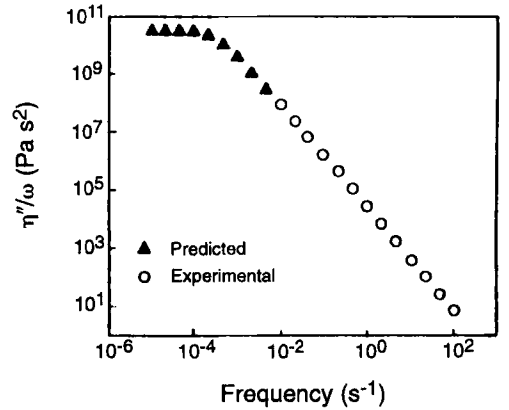

FIG. 29. Experimental and predicted values of η''/ω versus frequency for the 40% moisture hard flour dough sample (Dus and Kokini, 1990).

of correlation between experimental and predicted data. The performance of this prediction is better than those of the other functions.

The rheological properties of a number of commercial glutens have been examined and compared with their baking performance when reconstituted with starch and flour water soluble material. Figure 30 shows the relationship between loaf volume and the dynamic rheological properties G' and G'' for a range of glutens hydrated to 65% moisture. There is an obvious relationship in that dough with higher values of the storage and loss moduli have consistently lower loaf volumes (LeGrys *et al.*, 1981). Thus, for a gluten to perform well in a baking test it should be extensible without an excessive amount of elastic recoil.

D. RHEOLOGY OF EMULSIONS

Emulsions are dispersions of one liquid phase in the form of fine droplets in another immiscible liquid phase. The immisciable phases are usually oil and water, so emulsions can be broadly classified as oil-in-water or water-in-oil emulsions, depending on the dispersed phase. Some typical food emulsions are mild cream, ice cream, butter, margarine, salad dressing, and meat emulsions. The results from rheological measurements can allow for a better understanding of how various emulsifiers/stabilizers interact to stabilize emulsions. Understanding the effect of additives such as food

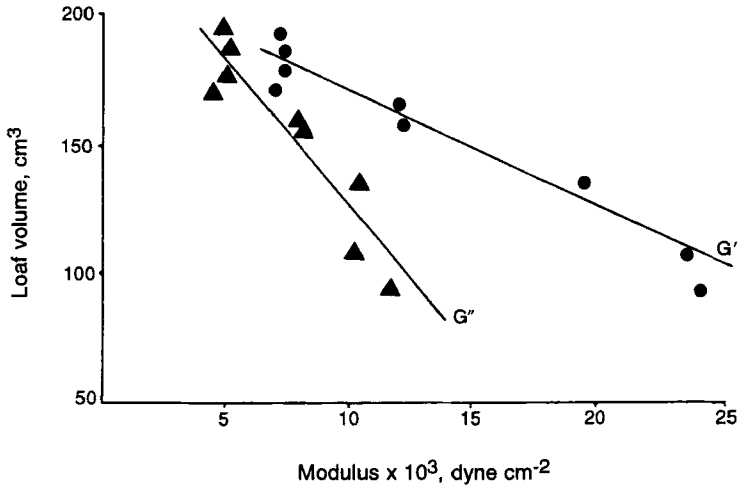

FIG. 30. Relationship between loaf volume and storage and loss moduli for commercial glutens rehydrated, after freeze drying, to 65% moisture (frequency = 10 rad/sec, strain = 0.25; LeGrys *et al.*, 1981).

gums, salts, and sugar on the stabilizing action emulsifiers/stabilizers allows the development of the best mixture of stabilizers to function effectively in food systems.

Steady shear measurements were used to determine flow properties and to estimate the degree of structure breakdown with shear (Elliott and Ganz, 1977). The power law equation (Eq. 3) has been used to describe the shear stress–shear rate behavior of salad dressings (Figoni and Shoemaker, 1983; Paredes *et al.*, 1988, 1989). The flow behavior index of five commercial salad dressings at different temperatures and storage times of up to 29 days were all less than one, indicating that they were pseudoplastic fluids. The consistency index (K) decreased with the increase in product temperature.

Shear modulus is a measure of the elasticity of an emulsion. The higher the shear modulus, the greater the capacity of an emulsion to store energy. In practice, a high value of shear modulus is indicative of enhanced emulsion stability in low-stress situations. On the other hand, high shear modulus usually implies high viscosity which also increases pumping and handling difficulties (Gladwell *et al.*, 1985a,b). It is also possible to link the shear modulus with colloidal interactions between droplets (Buscall *et al.*, 1982). In soy oil–water emulsions, most of the viscoelastic behavior can be attributed to the interactions between xanthan gum microgel and emulsion droplets, which indicates that the droplets behave as soft deformable spheres rather than as rigid spheres (Gladwell *et al.*, 1985a,b).

The compliance response of viscoelastic materials in a creep/recovery test is due to three mechanisms: instantaneous elastic, retarded elastic, and viscous flow. As oil concentration increases, the emulsions become more elastic, with the instantaneous elastic mechanism becoming more dominant. In the nonlinear region the viscous flow is more dominant, with the emulsions becoming less elastic with increasing shear stress (Gladwell *et al.*, 1985a,b). A four parameter model was employed to describe the creep compliance data (Paredes *et al.*, 1988). Major changes in the rheological parameters took place during the initial 7 days of storage. Egg yolk is used in food emulsions, such as salad dressing and mayonnaise, to lower the oil–water interfacial tension. Hydrocolloid gum such as propylene glycol alginate, carrageenan, guar, and xanthan are the main emulsion stabilizers in commercial salad dressings. Because of their complex composition (e.g., egg yolk, food gums, salt, etc.), salad dressings exhibit complex and thixotropic rheological properties (Paredes *et al.*, 1988). Vernon-Carter and Sherman (1980) reported that the creep was influenced by pH, electrolytes ($NaCl$, $CaCl_2$), and storage time. The change in rheological properties during storage was dependent on the rate of droplet coalescence and the ability of the mesquite layers in adjacent oil droplets to interpenetrate and form

new linkages. Table IX shows the magnitudes of the four creep parameters for the six salad dressings (Paredes *et al.*, 1988).

Structural breakdown is a time-dependent process resulting in a decrease in the viscosity of a product. The classical approach to characterizing structural breakdown is the measurement of the hysteresis loop, first reported by Green and Weltmann (1943). A sample is sheared at a continuously increasing, then continuously decreasing, shear rate, and a shear stress–shear rate flow curve is plotted. If structural breakdown occurs, the two curves do not coincide, creating a hysteresis loop. The area enclosed by the loop indicates the degree of breakdown.

Dynamic measurements, at strain amplitudes within the linear viscoelastic limit, were made to establish the properties of the essentially undisturbed samples (Elliott and Ganz, 1977). Oscillatory experiments are a powerful tool to study the effects of aging, the amount and type of ingredients, and additives such as food gums on the rheological properties and quality of salad dressings (Munoz and Sherman, 1990).

Small amplitude dynamic viscoelastic properties of apple butter, mustard, table margarine, and mayonnaise were compared to their respective properties in steady shear flow in the range of shear rates and frequencies of 0.1 to 100 sec^{-1} (Bistany and Kokini, 1983). Comparisons of dynamic and steady viscosities showed that dynamic viscosities (η^*) are much greater than steady viscosities (η). Consequently, the Cox–Merz rule is not obeyed (Bistany and Kokini, 1983). This phenomenon can be explained by a signifi-

TABLE IX

FOUR CREEP PARAMETERS OF SIX COMMERCIAL SALAD DRESSINGS[a]

Product	δ_r (dyne/cm^2)	E_0 (dyn/cm^2 $\times 10^{-3}$)	E_1 (dyn/cm^2 $\times 10^{-3}$)	η_1 (P $\times 10^{-3}$)	η_N (P $\times 10^{-3}$)
A[b]	55.2	1.42	1.0	16.2	79.8
ARC[c]	55.2	0.55	0.52	22.5	148.8
B[d]	55.2	2.04	2.08	38.5	587.4
BRC[e]	55.2	1.15	0.27	7.05	67.2
C[f]	22.8	0.62	1.02	9.10	19.8
D[g]	22.8	0.61	0.48	1.16	3.6

[a]Source: Paredes *et al.*, 1989.
[b]A is bottled creamy style A.
[c]ARC is bottled creamy style A—reduced calorie.
[d]B is bottled creamy style B.
[e]BRC is bottled creamy style B—reduced calorie.
[f]C is dry creamy mix style C.
[g]D is dry creamy mix style D.

cant destructive effect during the steady shear measurements. However, the structure breakdown due to shear strains between 0.001 and 0.1 was found to be fully recoverable in a small amplitude oscillatory test of butter (Rohm and Weidinger, 1993). No qualitative differences in the rheological behaviors were observed between the samples. Temperature-induced variations were mainly ascribed to changes in the solid fat content. Correlations between selected rheological measures in the linear viscoelastic region (i.e., complex modulus, G^*, relaxation modulus, $G(t)$, and modulus of deformability, Md) were affected by the solid fat content (Rohm and Weidinger, 1993).

Margarine and tablespread are oil-in-water emulsions. Melting characteristics of these products are important for flavor release and consumer acceptance. Oscillatory measurements as a function of temperature and drop points were used to quantify rheological changes accompanying melting. The rheology of low-fat spread is governed by emulsion characteristics such as the proportion of the aqueous phase and the size of the water droplets.

E. EXTENSIONAL FLOW

While shear rheological properties of food materials have received a great deal of attention (Kokini and Dickie, 1981; Plutchok and Kokini, 1986), extensional properties of food materials are only recently being investigated (Bagley *et al.*, 1988; Bagley, 1992a; Bhattacharya and Padmanabhan, 1992). Among the wide variety of food materials, wheat dough is one of the most complex and also the most interesting. Schofield and Scott-Blair (1932) studied the relaxation and elastic recovery of dough during extension and suggested that the elastic behavior of wheat dough resulted from the protein fraction of flour.

Hlynka and Anderson (1952) examined the relaxation behavior of dough in tension using a spectrum of relaxation times. They found that gluten relaxograms were of the same type as those of dough, but starch relaxograms were different from those of dough. Glucklich and Shelef (1962) showed wheat flour dough to be nonlinear viscoelastic in uniaxial compression past a critical stress value. They also noted that dough might be regarded as almost incompressible due to a very large elastic bulk modulus. Tschoegl *et al.* (1970a,b) confirmed nonlinear viscoelastic behavior in large deformation. They found that extension rate, temperature, water content, and flour type had a drastic effect on stress–strain behavior.

Bagley (1992a) measured the apparent biaxial elongational viscosity of wheat flour dough. The upper convected Maxwell model was considered to be adequate in explaining both the effect of crosshead speed and sample

dimensions. The Leonov constitutive model was also used by the same author in analyzing both extensional and shear flows.

Senouci and Smith (1988) used a simplified analysis for converging flow in a piston-driving capillary rheometer at 120–130°C and obtained ratios of uniaxial extensional viscosities to shear viscosities of maize grits and potato powder in the range of 60–3900.

Gas cell expansion for loaf volume development during baking is largely biaxial stretching flow (Bloksma and Nieman, 1975; de Bruijne *et al.*, 1990). Extensional viscosity data of wheat dough are necessary to relate functional properties of bread such as loaf volume to biaxial extensional rheological properties. Bloksma (1988) estimated that extensional rate ranged from 10^{-4} to 10^{-3} sec^{-1} during fermentation of bread dough. To predict the performance of these processes it is necessary to obtain accurate biaxial extensional viscosity data, preferably in this range of extension rate.

Doughs with different protein contents (13.2, 16.0, and 18.8% based on 14%MB) showed different biaxial extensional viscosities (Huang and Kokini, 1993). Figure 31 shows that the biaxial extensional viscosity approached 6η at an extensional rate of 7.3×10^{-5} sec^{-1}. Strain thinning behavior was observed in dough during biaxial extension.

F. FORMULATIONS DEVELOPMENT

Most food producers want to process at the highest rate possible for maximum output. However, the shear history during processing can

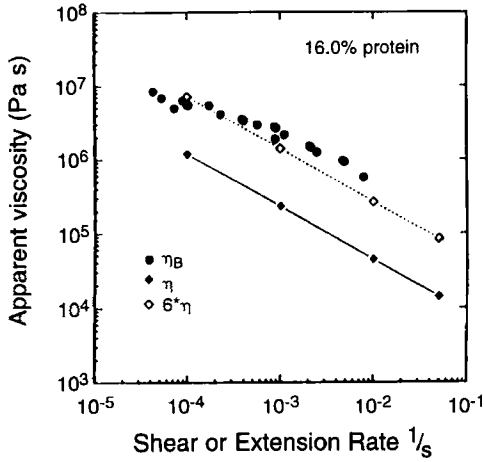

FIG. 31. Biaxial extensional viscosity and shear viscosity vs extension and shear for wheat flour dough with 16.0% protein content (Huang and Kokini, 1993). η_B is biaxial extensional viscosity. η is shear viscosity. $6^*\eta$ superimposed with η_B indicate that the biaxial extensional viscosity are about five times larger than shear viscosity at the equivalent shear rate.

change the fluid microstructure, which, in turn, may affect the characteristics of the final product. As consumers are becoming more concerned about health and nutrition, food researchers seek to adjust product formulations to reduce calories and still provide good quality. But it is important to fully compare ingredients before switching formulations, as some may appear the same but behave differently in processing. Figure 32a compares the results of three different starch solutions at 70°C, while Fig. 32b compares the same solutions at 130°C. Comparing the order of these three solutions based on the viscosity at the two temperatures shows that the order is reversed. The molecular weight and conformation of the starch molecules in solution have a great effect on the enhancement of the viscosity.

The gel point in materials represents the point where behavior changes from viscous (liquid-like) to elastic (solid-like). The conditions under which this occurs are critical to such food constituents as wheat–soya solutions used as setting agents within reconstituted meat products. In this case, oscillatory-controlled stress experiments, in which a small sinusoidal stress is applied to the material, provide a convenient method for evaluating elastic and viscous properties without destroying the delicate structure of soft semisolids.

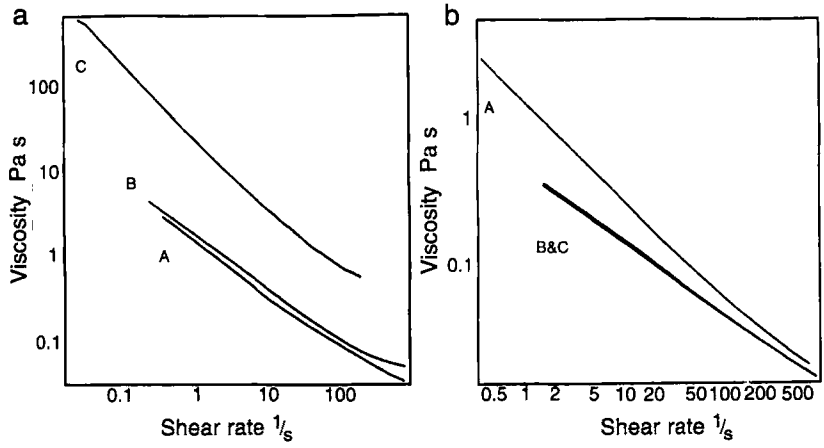

FIG. 32. Viscosity as a function of shear rate for three starch solutions (Race, 1993). A, starch solution A; B, starch solution B; C, starch solution C. (a) Measured at 70°C in the high pressure cell. (b) Measured at 130°C in the high pressure cell. Note that in (a) the viscosity was measured at 70°C, the starch solution A behaves similar to B but significantly smaller than starch solution C; in (b) the viscosity was measured at 130°C, the viscosity starch solution A was significantly greater than that of solution B and C, while solution B and C behaves in a similar way.

Figure 33 illustrates the ability to detect the temperature of gelation for two aqueous wheat solutions with different gelation enhancing enzymes. The temperature of gelation point is where the G' and G'' curves cross (G' and G'' being the storage and loss modulus, respectively, and the crossover point at which there is a balance between solid- and liquid-like structure). Even though the different enzymes yield the same gelling temperature, the final gel strength G' is much higher for enzyme A. This information can be used to gain an appreciation of the food product's behavior during production and when consumed. For example, at the gel point, the character of food changes significantly. Therefore, it may be crucial to pump products into packaging before this point is reached. The gel strength, on the other hand, has a great bearing on a texture of food, and, hence, the appeal when consumed. In the case of reconstituted meat products, gel strength also dictates whether or not they hold together during heating and cooking.

VII. SUMMARY AND RESEARCH NEEDS

An attempt has been made to review the essential food rheology concepts and the current state of knowledge regarding rheological properties of food materials and food products. The progress made in the measurement and simulation of the viscoelasticity of semisolid food and their biopolymeric

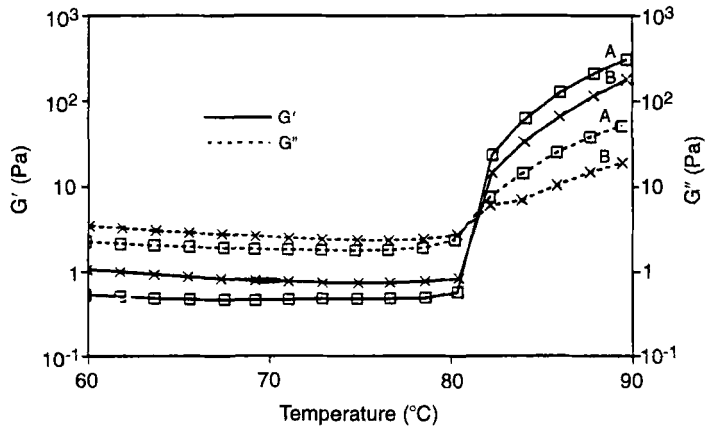

A: Wheat solution treated with enzyme A
B: Wheat solution treated with enzyme B

FIG. 33. Gelation of wheat solutions (Anonymous, 1993). A, wheat solution treated with enzyme A. B, wheat solution treated with enzyme B.

components has also been discussed. Various constitutive equations have been employed for the interpretation of experimental data and prediction of the rheological properties of food material and food products. In particular, constitutive models were shown to be useful in many ways.

First, dilute solution theories have been shown to be useful to characterize long range conformation and flexibility of carbohydrate- and protein-based polymers. Rheological measurements and constitutive theories predicting rheological properties compliment short range studies such as neutron scattering. One important advantage of combining short range vs long range studies was to understand the effect of short range flexibility on long range conformation. This would be a fertile area for new research.

Second, semiempirical constitutive models such as the Bird–Carreau model were shown to be useful to generate a database for predicting steady and small amplitude rheological properties of viscoelastic materials. This database should enable estimation of important parameters such as recoverable strain, which affects die swell and recovery processes in general in the processing of viscoelastic materials. While these models do not originate from specific molecular information, they do incorporate key assumptions pertaining to network formation and dissolution which clearly occurs during deformation processes. The semiempiricism facilitates the estimation of parameters and makes the model easily applicable to complex food material such as dough.

Third, a constitutive model with accurate molecular and conformational origins such as the Doi–Edwards model was able to simulate concentrated pectin dispersion rheology quite accurately. Such studies enabled correlation between chemical structure and functionality. While state of the art modeling does not permit the use of such detailed understanding with complex food systems, it nevertheless provides major clues about how to design molecules for functionality. Such knowledge can provide design guidelines to genetically engineer materials of biological origin with optimal functionality.

Clearly there is need for much more work in these areas of food rheology. It is first necessary to develop better methods for extensional viscosity of fluid and semigels. In addition, it is necessary to bring constitutive models into the field that are able to predict extensional properties. Constitutive models which can predict rheological properties of dispersed system (suspensions, emulsions) need to be developed. Advances in techniques and numerical methods are necessary so that nonlinear constitutive models can be developed that are capable of incorporating the diverse and complex structural properties of foods. The predictive capability developed through this effort will result in product design and process improvement rules leading to improved food products for the consumer.

REFERENCES

Ainsworth, P. A., and Blanshard, J. M. V. (1980). Effect of thermal processing on structure and rheological properties of carrageenan/carob gum gels. *J. Text. Stud.* **11,** 149–162.

Anonymous (1993). TA Instruments Application Notes.

Bagley, E. B. (1992a). Constitutive models for doughs. *In* "Food Extrusion Science and Technology" (J. L. Kokini, C. Ho, and M. V. Karwe, eds.), pp. 203–212. Dekker, New York.

Bagley, E. G., Christianson, D. D., and Martindale, J. A. (1988). Uniaxial compression of a hard wheat flour dough: Data analysis using the upper convected Maxwell model. *J. Text. Stud.* **19,** 289–305.

Barbosa-Cánovas, G. V., and Peleg, M. (1983). Flow parameters of selected commercial semiliquid food products. *J. Text. Stud.* **14,** 213–234.

Barbosa-Cánovas, G. V., Ibarz, A., and Peleg, M. (1993). Propiedades reológicas de alimentos fluidos. *Rev. Aliment.* **241,** 43–93.

Barnes, H. A., and Walters, K. (1985). The yield stress myth? *Rheol. Acta* **24,** 323–326.

Barnes, H. A., Hutton, J. F., and Walters, K. (1989). "An Introduction to Rheology." Elsevier, New York.

Bhattacharya, M., and Padmanabhan, M. (1992). On line rheological measurement of food dough during extrusion cooking. *In* "Food Extrusion Science and Technology" (J. L. Kokini, C. Ho, and M. V. Karwe, eds.), pp. 213–232. Dekker, New York.

Bird, R. B., and Carreau, P. J. (1968). A nonlinear viscoelastic model for polymer solutions and melts. I. *Chem. Eng. Sci.* **23,** 427–434.

Bird, R. B., Stewart, W. E., and Lightfoot, E. N. (1969). "Transport Phenomena." Wiley, New York.

Bird, R. B., Armstrong, R. C., and Hassager, O. (1977). "Dynamics of Polymeric Liquids." Wiley, New York.

Bird, R. B., Armstrong, R. C., and Hassager, O. (1987). Fluid dynamics of rheometry. "Dynamics of Polymer Liquids," 2nd ed., Vol. 1, Chapter 10. Wiley, New York.

Bistany, K. L., and Kokini, J. L. (1983). Comparison of steady shear rheological properties and small amplitude dynamic viscoelastic properties of fluid food materials. *J. Text. Stud.* **14,** 113–124.

Bloksma, A. H. (1972). Rheology of wheat flour doughs. *J. Text. Stud.* **3,** 3–17.

Bloksma, A. H. (1988). Rheological of the breadmaking process. *Pap., Int. Cereal Bread Congr., 8th,* Lausanne, Switzerland, 1988.

Bloksma, A. H., and Nieman, W. (1975). The effect of temperature on some rheological properties of wheat flour doughs. *J. Text. Stud.* **6,** 343.

Bourne, M. C. (1994). Covering from empirical to rheological tests on foods—it's a matter of time. *Cereal Foods World* **39**(1), 37–39.

Buscall, R., Goodwin, J. W., Hawkins, M. W., and Ottewill, R. H. (1982). Viscoelastic properties of concentrated lattices. Part 2. Theoretical analysis. *J. Chem. Soc., Faraday Trans. I* **78,** 2889.

Campanella, O. H., and Peleg, M. (1987b). Determination of the yield stress of semi-liquid foods from squeezing flow data. *J. Food Sci.* **52,** 214–215.

Campanella, O. H., and Peleg, M. (1987c). Analysis of the transient flow of mayonnaise in a coaxial cylinder viscometer. *J. Rheol.* **31,** 439–452.

Carreau, P. J., MacKonald, I. F., and Bird, R. B. (1968). A non linear viscoelastic model for polymer solutions and melts. Part 2. *Chem. Eng. Sci.* **23,** 901.

Charm, S. E. (1963). The direct determination of shear stress-shear rate behavior of foods in the presence of yield stress. *J. Food Sci.* **28,** 107–113.

Cheng, D. C. H. (1986). Yield stress: A time dependent properties and how to measure it. *Rheol. Acta* **25,** 25–554.

Cheng, D. C. H., and Evans, F. (1965). Phenomenological characterization of the rheological behavior of inelastic reversible thixotropic and antithixotropic fluid. *Br. J. Appl. Phys.* **16,** 1599–1617.

Chou, T. C., and Kokini, J. L. (1987). Rheological properties and conformation of tomato paste pectins, citrus and apple juice pectins. *J. Food Sci.* **52,** 1658.

Chou, T. C., Pintauro, N., and Kokini, J. L. (1991). Conformation of citrus pectin using small amplitude oscillatory rheometry. *J. Food Sci.* **56,** 1365–1371.

Cohen, Y., and Metzner, A. B. (1986). An analysis of apparent slip flow of polymer solutions. *Rheol. Acta* **25,** 28–35.

Connelly, R. W., and Greener, J. (1985). High-shear viscometry with a rotational parallel-disk device. *J. Rheol.* **29**(2), 209–226.

Crandall, P. G., Chen, C. S., and Carter, R. D. (1982). Models for predicting viscosity of orange juice concentrates. *Food Technol.* **36**(5), 245.

Cross, M. M. (1965). Rheology of non-Newtonian fluid: A new flow equation for pseudoplastic systems. *J. Colloid Sci.* **20,** 417–437.

Darby, R. (1976). "Viscoelastic Fluids: An Introduction to their Properties and Behavior." Dekker, New York.

Dealy, J. M., and Wissbrun, K. F. (1990). "Melt Rheology and Its Role in Plastics Processing." Van Nostrand-Reinhold, New York.

de Bruijne, D. W., de Looff, J., and van Eulem, A. (1990). The rheological properties of bread dough and their relation to baking. *In* "Rheology of Food, Pharmaceutical and Biological Materials with General Rheology" (R. E. Carter, ed.), pp. 269–283. Elsevier, New York.

De Kee, D., Turcotte, G., and Fildey, K. (1980). New method for the determination of yield stress. *J. Text. Stud.* **10,** 281.

DeMan, J. M., ed. (1976). "Rheology and Texture in Food Quality." Avi Publ. Co., Westport, CT.

de Vargas, L., Perez-Gonzalez, J., and Romero-Barenque, J. D. (1993). Experimental evidence of slip development in capillaries and a method to correct for end effects in the flow of xanthan solution. *J. Rheol.* **37**(5), 867–878.

Dickie, A., and Kokini, J. L. (1982). Use of the Bire-Leider equation in food rheology. *J. Food Process. Eng.* **5,** 157–174.

Doi, E., and Edwards, R. H. (1978). *J. Chem. Soc., Faraday Trans. 2* **74,** 1789.

Doi, E., and Edwards, R. H. (1979). *J. Chem. Soc., Faraday Trans. 2* **75,** 38.

Doi, E., and Edwards, R. H. (1986). "The Theory of Polymer Dynamics." Oxford Univ. Press, Oxford.

Doublier, J. L., and Launay, B. (1976). Rheological properties of galactomannan in aqueous solutions: Effect of concentration and molecular weight. *Proc. Int. Congr. Rheol., 6th,* pp. 532–533.

Doublier, J. L., and Launay, B. (1981). Rheological galactomannan solutions: Comparative study of guar gum and locust bean gum. *J. Text. Stud.* **12,** 151–172.

Drake, M. A., Ma, L., Swanson, B. G., and Barbosa-Cánovas, G. V. (1994). Rheological characteristics of milkfat and milkfat blend sucrose polyesters. *Food Res. Int.* **27,** 477.

Dus, S. J., and Kokini, J. L. (1990). Prediction of the non-linear viscoelastic properties of a hard wheat flour dough using the Bird-Carreau constitutive model. *J. Rheol.* **34**(7), 1069–1084.

Elliott, J. H., and Ganz, A. J. (1977). Research note: Salad dressing—Preliminary rheological characterization. *J. Text. Stud.* **8,** 359–371.

Escher, F. (1983). Relevance of rheological data in food processing. *In* "Physical Properties of Foods" (R. Jowitt, F. Escher, B. Hallström, H. T. Th. Meffert and G. Vos, eds.), pp. 103–110. Applied Science, New York.

Evans, I. D. (1992). Letter to editor: On the nature of the yield stress. *J. Rheol.* **36**(7), 1313–1316.

Fernández-Martín, F. (1972). Influence of temperature and composition on some physical properties of milk concentrates. I. Viscosity. *J. Dairy Res.* **39,** 75.

Ferry, J. D. (1980). "Viscoelastic Properties of Polymers." Wiley, New York.

Figoni, P. I., and Shoemaker, C. F. (1983). Characterization of time dependent flow properties of mayonnaise under steady shear. *J. Text. Stud.* **14,** 431–442.

Frederickson, A. G. (1964). "Principles and Applications of Rheology." Prentice-Hall, New York.

Gencer, G. K. (1985). Interactions of selected gums in solution and the effect of common food ingredients on these interactions. Ph.D. Dissertation, University of Massachusetts, Amherst.

Gladwell, N., Rahalkar, R. R., and Richmond, P. (1985a). Rheological behavior of soya oil water emulsion: Dependence upon oil concentration. *J. Food Sci.* **50,** 440–443.

Gladwell, N., Rahalkar, R. R., and Richmond, P. (1985b). Creep/recovery behavior of oil-water emulsions: Influence of disperse phase concentration. *J. Food Sci.* **50,** 1477–1481.

Glucklich, J., and Shelef, L. (1962). An investigation into the rheological properties of flour dough: Studies in shear and compression. *Cereal Chem.* **39,** 243–255.

Gould, W. A. (1983). "Tomato Production, Processing and Quality Evaluation," 2nd ed. Avi Publ. Co., Westport, CT.

Green, H., and Weltmann, R. N. (1943). Analysis of the thixotropy of pigment vehicle suspensions: Basic principles of the hysteresis loop. *Ind. Eng. Chem., Anal. Ed.* **15,** 201–206.

Harper, J. C. (1960). Viscometric behavior in relation to evaporation of fruit purees. *Food Technol.* **14,** 557–561.

Harris, J. (1972). A continuum theory of structural change. *Rheol. Acta* **11,** 145–151.

Hartnett, J. P., and Hu, R. Y. Z. (1989). Technical note: The yield stress—an engineering reality. *J. Rheol.* **33**(4), 671–679.

Hibberd, G. E., and Wallace, W. J. (1966). Dynamic viscoelastic behavior of wheat flour doughs. Part I. Linear aspects. *Rheol. Acta* **5,** 193–198.

Higgs, S. D. (1974). An investigation into the flow behavior of complex non-Newtonian foodstuffs. *J. Phys. D* **7,** 1184–1191.

Hlynka, I., and Anderson, J. A. (1952). Relaxation of tension in stretched dough. *Can. J. Tech.* **30,** 198.

Huang, H., and Kokini, J. L. (1993). Measurement of biaxial extensional viscosity of wheat flour doughs. *J. Rheol.* **37,** 879–891.

Ibarz, A., Vicente, M., and Graell, J. (1987). Rheological behavior of apple juice and pear juice and their concentrates. *J. Food Eng.* **6,** 257–267.

Ibarz, A., Pagan, J., Guitierrez, J., and Vicente, M. (1989). Rheological properties of clarified pear juices concentrates. *J. Food Eng.* **10,** 57–63.

Ibarz, A., Gonzalez, C., Esplugas, S., and Vicente, M. (1992). Rheology of clarified fruit juices. I. Peach juices. *J. Food Eng.* **15,** 49–61.

Kee, De D., and Durning, C. J. (1990). Rheology of materials with a yield stress. *In* "Polymer Rheology and Processing" (A. A. Collyer and L. A. Utracki, eds.). Elsevier, New York.

Kirkwood, J. G., and Auer, P. L. (1951). The visco-elastic properties of solutions of rod-like macromolecules. *J. Chem. Phys.* **19,** 281–283.

Kokini, J. L. (1992). Rheological properties of foods. *In* "Handbook of Food Engineering" (D. R. Heldman and D. B. Lund, eds.), 1st ed. Dekker, New York.

Kokini, J. L. (1993). Constitutive models for dilute and concentrated food biopolymer systems. *In* "Plant Polymeric Carbohydrates" (F. Meuser, D. J. Manners, and W. Seibel, eds.), pp. 43–75. Royal Society of Chemistry, Cambridge, UK.

Kokini, J. L., and Chou, T. C. (1993). Comparison of the conformation of tomato pectins with apple and citrus pectins. *J. Text. Stud.* **24,** 117–137.

Kokini, J. L., and Dickie, A. (1981). An attempt to identify and model transient viscoelastic flow in foods. *J. Text. Stud.* **12,** 539–557.

Kokini, J. L., and Plutchok, G. J. (1987a). Predicting steady and oscillatory shear rheological properties of cmc/guar blends using the Bird-Carreau constitutive model. *J. Text. Stud.* **18,** 31–42.

Kokini, J. L., and Plutchok, G. J. (1987b). Viscoelastic properties of semisolid foods and their biopolymeric components. *Food Technol.* **41**(3), 89–95.

Kokini, J. L., Bistany, K. L., and Mills, P. L. (1984). Predicting steady shear and dynamic viscoelastic properties of guar and carrageenan using the Bird-Carreau constitutive model. *J. Food Sci.* **49,** 1569–1576.

Konstance, R. P., and Holsinger, V. H. (1992). Development of rheological test methods for cheese. *Food Technol.* **46**(1), 105–109.

Lang, E. R., and Rha, C. (1981). Determination of the yield stress of hydrocolloid dispersions. *J. Text. Stud.* **12,** 47.

Launay, B., and Pasquet, E. (1982). Interaction of hydrocolloids. *In* "Gums and Stabilizers for Food Industry 1" (G. O. Phillips, D. J. Wedlock, and P. A. Williams, eds.). Elsevier, New York.

LeGrys, G. A., Booth, M. R., and Al-Baghdadi, S. M. (1981). The physical properties of wheat proteins. *In* "Cereals: A Renewable Resource" (Y. Pomeranz and L. Munck, eds.). AACC, St. Paul, MN.

Leider, P. J., and Bird, R. B. (1974). Squeezing flow between parallel disks. I. Theoretical analysis. *Ind. Eng. Chem. Fundam.* **113,** 336–341.

Leppard, W. R. (1975). Viscoelasticity: Stress measurements and constitutive theory. Ph.D. dissertation, University of Utah, Salt Lake City.

Liguori, C. A. (1985). The relationship between the viscoelastic properties and the structure of sodium alginate and propylene glycol alginate. M. S. Thesis, Rutgers University, New Brunswick, NJ.

Ma, L., and Barbosa-Cánovas, G. V. (1995a). Rheological characterization of mayonnaise. Part I. Slippage at different oil and xanthan gum concentrations. *J. Food Eng.* **25,** 397–408.

Ma, L., and Barbosa-Cánovas, G. V. (1995b). Rheological characterization of mayonnaise. Part II. Flow and viscoelastic properties at different oil and xanthan gum concentrations. *J. Food Eng.* **25,** 409–425.

Marvin, R. S., and McKinney, J. E. (1965). *In* "Physical Acoustice" (W. P. Mason, ed.), Vol. B. Academic Press, New York.

Mason, P. L., Bistany, K. L., Puoti, M. G., and Kokini, J. L. (1982). A new empirical model to simulate transient shear stress growth in semi-solid foods. *J. Food Process. Eng.* **6,** 219–33.

Mewis, J. (1979). Thixotropy—A general review. *J. Non-Newtonian Fluid Mech.* **6,** 1–20.

Missaire, F., Qiu, C.-G., and Rao, M. A. (1990). Yield stress of structured and unstructured food suspensions. *J. Text. Stud.* **21,** 479–490.

Mitchell, J. R. (1979). "Rheology of Polysaccharides Solutions and Gels. Polysaccharides in Food." Butterworth, London.

Mooney, M. (1931). Explicit formulas for slip and fluidity. *J. Rheol.* **2,** 210–222.

Muller, H. G. (1973). "An Introduction to Food Rheology." Crane, Russak & Co., New York.

Munoz, J., and Sherman, P. (1990). Dynamic viscoelastic properties of some commercial salad dressing. *J. Text. Stud.* **21,** 411–426.

Navickis, L. L., and Bagley, E. B. (1983). Yield stresses in concentrated dispersions of closely packed, deformable gel particles. *J. Rheol.* **27**(6), 519–536.

Nussinovitch, A., Peleg, M., and Normand, M. D. (1989). A modified Maxwell and a nonexponential model for characterization of the stress relaxation of agar and alginate gel. *J. Food Sci.* **54,** 1013–1015.

Oakenfull, D., and Scott, A. (1988). Size and stability of the junction zones in gels of iota and kappa carrageenan. *In* "Gums and Stabilizers for Food Industry 4" (G. O. Phillips, D. J. Wedlock, and P. A. Williams, eds.). Elsevier, New York.

Ofoli, R. Y., Morgan, R. G., and Steffe, J. F. (1987). A generalized rheological model for inelastic fluid foods. *J. Text. Stud.* **18,** 213–230.

Paredes, M. D. C., Rao, M. A., and Bourne, M. C. (1988). Rheological characterization of salad dressings. 1. Steady shear, thixotropy and effect of temperature. *J. Text. Stud.* **19,** 247–258.

Paredes, M. D. C., Rao, M. A., and Bourne, M. C. (1989). Rheological characterization of salad dressing. 2. Effect of storage. *J. Text. Stud.* **20,** 235–250.

Peleg, M. (1977). Operational conditions and the stress strain relationship of solid foods—theoretical evaluation. *J. Text. Stud.* **8,** 283–295.

Plutchok, G. J., and Kokini, J. L. (1986). Predicting steady and oscillatory shear rheological properties of CMC and guar gum blends from concentration and molecular weight data. *J. Food Sci.* **51,** 1284–1288.

Princen, H. M. (1986). A novel design to eliminate end effects in concentric viscometer. *J. Rheol.* **30,** 271–283.

Prud'homme, R. K. (1991). Rheological measurement. *In* "Polymers as Rheology Modifiers" (D. N. Schulz and J. E. Glass, eds.). Maples Press, New York.

Qiu, C. G., and Rao, M. A. (1988). Role of pulp content and particle size in yield stress of apple sauce. *J. Food Sci.* **53,** 1165–1170.

Qui, C. G., and Rao, M. A. (1989). Effect of dispersed phase on the slip coefficient of apple sauce in a concentric cylinder viscometer. *J. Texture Stud.* **20,** 57–70.

Qui, C. G., and Rao, M. A. (1990). Quantitative estimates of slip of food suspensions in a concentric cylinder viscometer. *In* "Engineering and Food," (W. E. L. Spiess and H. Schubert, eds.), Vol. 1. Elsevier, New York.

Race, S. W. (1993). Bohlin Instruments Application Notes No. 7.

Rahalkar, R. R., Javanaud, C., Richmond, P., Melville, I., and Pethrick, R. A. (1985). Oscillatory shear measurements on concentrated dextran solutions: Comparison with Doi and Edwards' theory reptation. *J. Rheol.* **29**(6), 955–970.

Rani, U., and Bains, G. S. (1987). Flow behavior of tomato ketchups. *J. Text. Stud.* **18,** 125–135.

Rao, M. A., and Cooley, H. J. (1983). Applicability of flow models with yield of tomato concentrates. *J. Food Process. Eng.* **6,** 159–173.

Rao, M. A., Bourne, M. C., and Cooley, H. J. (1981). Flow properties of tomato concentrates. *J. Text. Stud.* **12,** 521–538.

Rao, M. A., Colley, H. J., and Vitali, A. A. (1984). Flow properties of concentrated juices at low temperatures. *Food Technol.* **38**(3), 113–119.

Rha, C. K. (1978). Rheology of fluid foods. *Food Technol.* **7,** 32–35.

Rohm, H., and Weidinger, K. H. (1993). Rheological behavior of butter at small deformations. *J. Text. Stud.* **24,** 157–172.

Rosenberg, M., Wang, Z., Chuang, S. L., and Shoemaker, C. F. (1995). Viscoelastic property changes in cheddar cheese during ripening. *J. Food Sci.* **60**(3), 640–644.

Rouse, P. E. (1953). A theory of the linear viscoelastic properties of dilute solutions of coiling polymer. *J. Chem. Phys.* **21,** 1272.

Saravacos, G. D. (1970). Effect of temperature on viscosity of fruit juices and purees. *J. Food Sci.* **35,** 122.

Schofield, R. K., and Scott-Blair, G. W. (1932). The relationship between viscosity, elasticity and plastic strength of soft materials as illustrated by some mechanical properties of flour doughs. *Proc. R. Soc. London, Ser. A* **138,** 707–717.

Schurz, J. (1992). Letter to the editor: A yield value in a true solution. *J. Rheol.* **36**(7), 1319–1321.

Senouci, A., and Smith, A. C. (1988). An experimental study of food melt rheology. II. End pressure effects. *Rheol. Acta* **27,** 649–655.

Shama, F., and Sherman, P. (1966). The texture of ice cream. II. Rheological properties of frozen ice cream. *J. Food Sci.* **31,** 699–716.

Sherman, P. (1970). "Industrial Rheology with Particular Reference to Foods, Pharmaceuticals and Cosmetics." Academic Press, New York.

Shoemaker, C. F., Lewis, J. I., and Tamura, M. S. (1987). Instrumentation for rheological measurements of food. *Food Technol.* **41**(3), 80.

Shrimanker, S. H. (1989). M. S. Thesis, Rutgers University, New Brunswick, NJ.

Smith, J. R., Smith, T. L., and Tschoegl, N. W. (1970). Rheological properties of wheat flour doughs. III. Dynamic shear modulus and its dependence on amplitude, frequency and dough composition. *Rheol. Acta* **9,** 239–252.

Steffe, J. F. (1992a). Yield stress: Phenomena and measurement. *In* "Advances in Food Engineering" (R. P. Singh and M. A. Wirakartakusumah, eds.), pp. 363–376. CRC Press, London.

Steffe, J. F. (1992b). Viscoelasticity. *In* "Rheological Methods in Food Process Engineering" (J. F. Steffe, ed.), 1st ed., pp. 168–194. Freeman Press, East Lansing, MI.

Steffe, J. F., Mohamed, I. O., and Ford, E. Q. (1986). Rheological properties of fluid foods: Data compilation. *In* "Physical and Chemical Properties of Food" (M. R. Okos, ed.), ASAE Publ., p. 1. *Am. Soc. Agric. Eng.,* St. Joseph, MI.

Struebi, P., Escher, F., and Neukom, H. (1978). Use of macerating pectic enzyme in apple nectar processing. *J. Food Sci.* **43,** 260.

Szczesniak, A. S. (1977). Rheological problems in the food industry. *J. Text. Stud.* **8,** 119.

Tiu, C., and Boger, D. V. (1974). Complete rheological characterization of time dependent food products. *J. Text. Stud.* **5,** 329–338.

Tschoegl, N. W., Rinde, J. A., and Smith, T. L. (1970a). Rheological properties of wheat flour doughs. I. Method for determining the large deformation and rupture properties in simple tension. *J. Sci. Agric.* **21,** 65–70.

Tschoegl, N. W., Rinde, J. A., and Smith, T. L. (1970b). Rheological properties of wheat flour doughs. II. Dependence of large deformation and rupture properties in simple tension on time, temperature and water absorption. *Rheol. Acta* **9,** 223–238.

Ullman, R. (1969). The viscoelastic properties of solutions of rod-like macromolecules of finite diameter. *Macromolecules* **2**(1), 27–30.

Vernon-Carter, E. J., and Sherman, P. (1980). Rheological properties and applications of mesquite tree (*Prosopis julifora*) gum. 2. Rheological properties and stability of o/w emulsions containing mesquite gum. *J. Text. Stud.* **11,** 351–365.

Vitali, A. A., and Rao, M. A. (1984). Flow properties of low pulp concentrated orange juice: Effect of temperature and concentration. *J. Food Sci.* **49,** 882–888.

Walters, K. (1975). "Rheometry." Chapman & Hall, London.

Whorlow, R. W. (1980). "Rheological Techniques." Wiley, New York.

Yamakawa, H. (1975). Viscoelastic properties of straight cylindrical macromolecules in dilute solutions. *Macromolecules* **8,** 339–342.

Yoshimura, A. S., Prud'homme, R. K., Princen, H. M., and Kiss, A. D. (1987). A comparison of techniques for measuring yield stresses. *J. Rheol.* **31**(8), 699–710.

Yoshimura, A. S., and Prud'homme, R. K. (1988). Wall slip corrections for couette and Parallel disk viscometers. *J. Rheol.* **32**(1), 53–67.

Zimm, B. H. (1956). Dynamics of polymer molecules in dilute solutions: Viscoelasticity, flow birefrigence and dielectric loss. pp. 241–269.